9950-722

SC5210.51FR

SC5210.51FR

Copy No. 2

III-V SEMICONDUCTOR SOLID SOLUTION SINGLE CRYSTAL GROWTH

FINAL REPORT FOR THE PERIOD
April 6, 1979 through April 16, 1981

SUBCONTRACT NO. 955352

Prepared for

California Institute of Technology
Jet Propulsion Laboratory
4800 Oak Grove Dr.
Pasadena, CA 91103

E.R. Gertner
Principal Investigator
Rockwell International Science Center
1049 Camino Dos Rios
Thousand Oaks, California 91360

FEBRUARY 1982

"This work was performed for the Jet Propulsion Laboratory, California Institute of Technology sponsored by the National Aeronautics and Space Administration under Contract NAS7-100."

"This report contains information prepared by Rockwell International Corporation under JPL sub-contract. Its content is not necessarily endorsed by the Jet Propulsion Laboratory, California Institute of Technology, or the National Aeronautics and Space Administration."

Rockwell International
Science Center

TABLE OF CONTENTS

LIST OF FIGURES

LIST OF FIGURES

LIST OF TABLES

FOREWORD

The work reported in this document was performed at the Rockwell International Science Center, Thousand Oaks, California for the National Aeronautics and Space Administration with the support of the California Institute of Technology, Jet Propulsion Lab, Pasadena, California under Subcontract number 955352. The monitoring engineer is Dr. J. Zoutendyk.

The principal investigators are E.R. Gertner and M.D. Lind with additional technical support provided by R.A. Reidel. The program manager is W.E. Tennant.

ABSTRACT

Research has been performed to determine the feasibility and desirability of space growth of bulk IR semiconductor crystals for use as substrates for epitxial IR detector material. Both a III-V ternary compound (GaInSb), and a II-VI binary compound have been considered. Conclusions are (1) vapor epitaxy and quaternary epitaxy techniques will be sufficient to permit the use of ground based binary III-V crystals for all major device applications; (2) float zoning of CdTe may eventully be a successful approach to obtaining high quality substrate material, but further experiments are required to verify this possibility.

1.0 INTRODUCTION

1.1 Motivation

The motivation for this program lies in the fact that while highest device performance is often demonstrated in epitaxial material ultimate device performance is often limited by the quality of the substrate material upon which the epitaxial material is deposited. Gravity is the one cause that limits the quality of current substrate material. While gravity effects both epitaxial and bulk single crystal growth processes its effect is much more pronounced in the bulk growth processes since epitaxial growth processes are typically confined to thin layers and short growth times. Gravity has a range of deleterious effects in bulk growth processes. They range from periodic doping variations to compositional inhomogeneities caused by convective flow. Also, the presence of gravity excludes the use of the float zoning technique for materials whose values of surface tension and density do not allow a stable liquid zone in a normal gravity environment. This class of material includes all of the III-V and II-VI solid-solution materials where the use of float zoning may be essential to achieve large, uniformly doped and compositionally homogeneous single crystals. In general, the use of a low gravity environment for crystal growth would have two benefits - first, material quality improvements for crystals presently grown in normal gravity and second, potential synthesis of crystals via growth techniques which can not be used in normal gravity.

1.2 Material Selection

For this program initially two material systems were considered - the III-V and II-VI compounds and solid solutions. While the II-VI system has greater versatility in the infrared detection area the III-V system has a much broader applications base with a variety of devices, such as lasers, LEDs, microwave and avalanche photodiodes, solar cells, and infrared detectors being fabricated in various III-V compounds and solid-solutions. Because of this wide application base we initially chose the III-V system in which to perform the low gravity growth experiments. Other considerations which supported this initial choice were the high stoichiometry typical of most III-V compound material - qualities important for device fabrication. Furthermore, the III-V solid-solutions were selected because of the relatively high quality and availability of commercially grown III-V binary compounds.

For device technology spanning the IR-visible range, it would be desirable to have lattice matching substrate materials continuously spanning the entire range of lattice parameters and energy gaps from GaP or AlP to InSb shown in Fig. 1. At present, the only III-V materials available in the size and quality required for use as substrates are the binary compounds, and cases of substantial lattice misfit are encountered. Because of this limitation, some device concepts are presently not feasible. Thus, there was at the onset of this program a strong motivation for attempting to grow bulk crystals of III-V solid solutions to provide lattice matching for any desired epitaxial structure.

Figure 2 shows calculated pseudobinary phase diagrams for the III-V solid solutions. The relatively large separations between the liquidus and

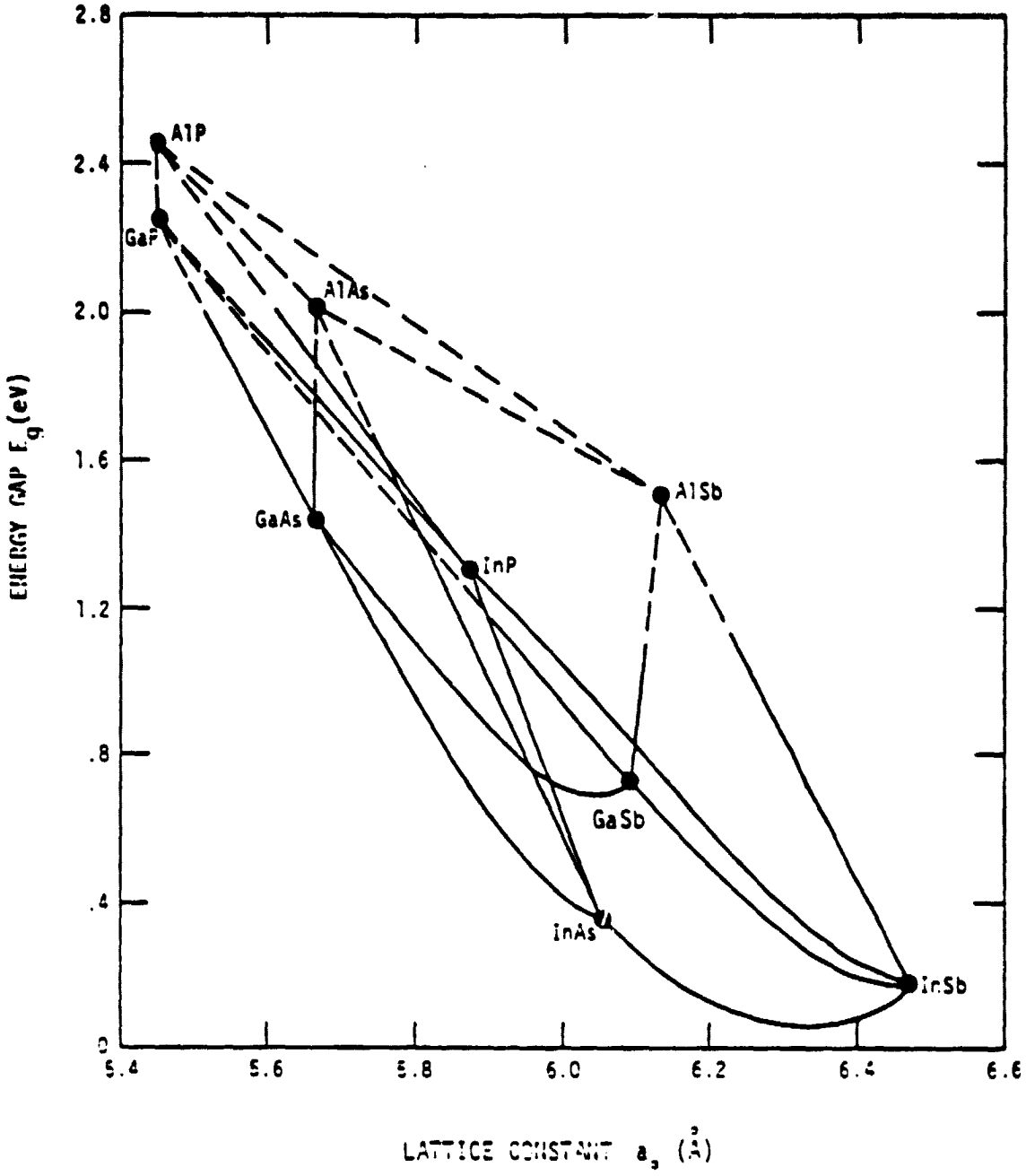

Fig. 1 Energy gap versus lattice constant for all III-V solid-solutions.

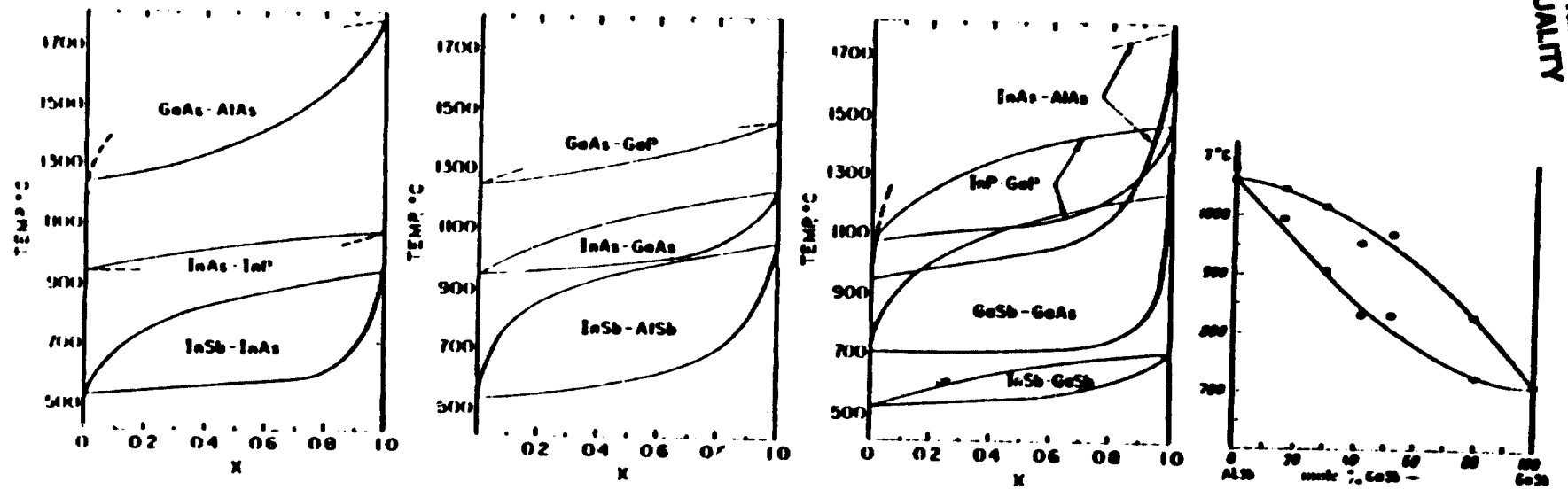

REF. - L. M. FOSTER, "THE PREPARATION OF III-V COMPOUND SEMICONDUCTOR ALLOYS" IN PREPARATION AND PROPERTIES OF SOLID STATE MATERIALS, VOL. 3, W. R. WILCOX AND R. A. LEFEVER, EDS, MARCEL DECKER, INC., NEW YORK, 1977; N. A. GORYUNOVA, "THE CHEMISTRY OF DIAMOND-LIKE SEMICONDUCTORS", MIT PRESS, CAMBRIDGE, MA, 1965.

Fig. 2 Pseudobinary phase diagram for III-V solid-solutions.

solidus and the relatively small slopes of portions of the curves in each of the diagrams are the primary reasons for the difficulty in growing solid solution single crystals, and reasonably large, compositionally homogeneous, strain free crystals have not been successfully synthesized in a normal gravity environment despite a variety of attempts by numerous investigators.

Although this initial choice of III-V alloys was well-justified, during the course of the program a reevaluation of this decision was made in the light of the rapid progress of alternative methods for the growth of III-V materials. The decision was made to switch from the growth of III-V to II-VI compounds. The explanation for this change is given later in this report.

The first part of the report therefore details the results of the original approach. This is followed by a description of the work accomplished on the growth of CdTe, which was the II-VI material selected for the remainder of this effort. CdTe is herein referred to as the "alternative approach".

1.3 Original Approach

The baseline approach for the III-V crystal growth experiments is a float zone technique in a low gravity environment. The two main risk areas in the single crystal growth of III-V solid solutions are growth problems due to the separation of liquidus and solidus and lattice mismatch. The technical problem therefore is to develop a growth technique for the single crystal growth of III-V solid-solutions.

The floating zone is a derivative of the zone melting technique first proposed by Pfann.[1] A molten zone is established at one end of an ingot and is passed through the ingot by moving it or the heating element. The molten zone

is maintained by the surface tension of the material. If a seed is provided at one end of the ingot, and care is taken not to melt the seed by the molten zone, the entire ingot can be grown as a single crystal. A substantial amount of the commercially available silicon is grown by this technique.

The float zone technique is ideally suited for the growth of the III-V solid-solutions because of three key aspects. First, it is capable of producing homogeneous crystals since growth occurs at constant temperature with continued replenishment of the liquid by the dissolving feed ingot. This aspect is very important since compositionally graded III-V solid-solution material will suffer from severe strain because of lattice-mismatch. Second, zone dimensions are reasonable with respect to solute diffusion rates since the maximum growth rates are determined by the diffusion of solute through the liquid zone thus smaller zones allow higher growth rates. Third, the technique is containerless which is an important consideration in the III-V solid-solution growth since many III-V compounds and solid-solutions expand upon solidification. Use of a container often results in higher dislocation densities, strain and in severe cases poly-crystallinity - all caused by varying degrees of "keying" or "wetting" of the containers by the liquid. Containerless growth also eliminates the possibility of contamination by chemical reaction between liquid and container.

There are two main reasons for the requirement of a low gravity environment for the float zone growth experiments - liquid zone stability and elimination of convection. Using Heywang's[2] criteria for the maximum zone length in normal gravity, we find for the $Ga_{.5}In_{.5}Sb$ case a length of approximately seven mm - half the length of that for silicon because of the lower surface tension and higher densities of the III-V compounds. Maintaining such short zone length

with reasonable crystal diameter is difficult and to our knowledge no successful float-zoning of any III-V compounds or solid-solution has been accomplished as yet in normal gravity. Liquid zone stability therefore is the first reason for a low gravity environment and the elimination of convection the second major reason. In crystal growth from solution, there always exists a boundary layer in front of the freezing interface which is either rich or depleted in constituents other than the material being grown. The concentration of these "impurities" depends on their individual distribution coefficients.

In the melt, however, there exist thermal gradients because the thermal conductivity of the liquid is not infinite. These thermal gradients give rise to density variation and the action of gravity on these density variations results in convection. Convection in turn, disturbs the boundary layer at the liquid-solid interface which causes non-uniform incorporation of impurities. Using appropriate chemical etches on cross-sections of grown crystals, these variations in impurity incorporation show up as growth "striations" or "bands" and are well documented in the open literature.[3,4] Examples for $InAs_{1-x}Sb_x$ and $Ga_{1-x}In_xSb$ grown by liquid phase epitaxy at the Science Center, are shown in Fig. 3. In a multi-component system, such as a III-V solid-solution, where liquid and solid are of very different composition, convection not only results in impurity striations, but also in compositional variations. If the end members of the solid-solution are lattice mismatched, compositional variations cause severe strain in the grown crystal. Because of the above considerations of zone stability without containers and elimination of convection, the absence of gravity is a requirement for the successful growth of single crystal III-V solid-solution.

SC78-1397

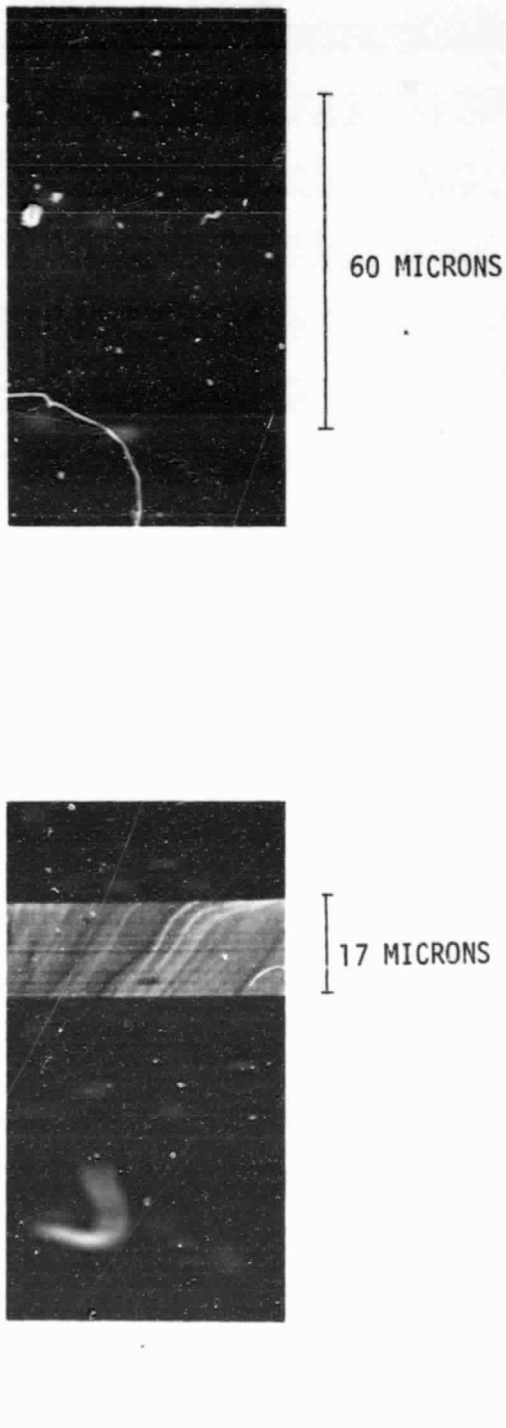

Fig. 3 Growth striations in $Ga_{1-x}In_xSb$ and $InAs_{1-x}Sb_x$.

For the initial growth experiments the $Ga_{1-x}In_xSb$ system was chosen because it has the lowest melting point and lowest vapor pressure of all the III-V systems. An outline of the initial floating zone experiments for $Ga_{1-x}In_xSb$ is shown in Fig. 4, together with the pseudobinary phase diagram. Two source rods of composition B, the solidus composition, are precast as homogeneously as possible. The floating zone, composition A, is also precast, since it is solid at room temperature, and sandwiched between the two source rods. A seed of composition B is placed at the end of one source rod. The growth cycle is initiated by melting the zone and moving it through the source rod toward the seed in order to ensure equilibrium between liquid zone and solid. Once the seed is reached by the liquid zone and properly wetted, the direction of zone movement is reversed and single crystal growth initiated. Use of a seed is essential to achieve single crystal growth since III-V compounds rarely self-nucleate without grains and recrystallization is virtually nil because of low interdiffusion coefficients in the solid phase. This brings us to the original objective of this program - the generation of $Ga_{1-x}In_xSb$ seed crystals for future low gravity growth experiments.

1.4 Original Objective

Following are the original objectives as taken from the work statement.

Task I -Perform initial seed growth and floating zone growth of gallium indium antimonide ($Ga_{1-x}In_xSb$) solid-solutions, using existing equipment.

SC78-1379

Fig. 4 Float zone experiment for $Ga_{1-x}In_xSb$.

Task II -Prepare a preliminary design for a second generation floating zone apparatus, using data from Task I.

Task III -Perform ground-based (normal gravity) experiments in support of low-gravity (space) floating zone growth of $Ga_{1-x}In_xSb$ solid-solutions.

To generate the seeds we proposed the liquid phase epitaxy (LPE) technique followed by a solute transport technique to increase the thickness of the epitaxial deposit since typical epitaxial layers are too thin to be useful as seeds for the floating zone technique since the molten zone has to "wet," that is, dissolve part of the seed in order to ensure good nucleation.

2.0 TECHNICAL APPROACH AND RESULTS

2.1 Epitaxial Growth of $Ga_{1-x}In_xSb$

$Ga_{1-x}In_xSb$ is lattice mismatched which dictates the use of special epitaxial growth processes to obtain high quality material. These techniques are illustrated in Fig. 5. To relieve the lattice mismatch the material must either be compositionally step graded or linearly graded. In linear graded material the misfit dislocation density is proportional to the compositional grading requiring thick layers to achieve low dislocation densities. In step grading an initial set of misfit dislocation is generated which then "thread" in and out at subsequent abrupt compositional steps relieving the strain of lattice mismatch. Ideally, no other misfit dislocation needs to be generated at subsequent interfaces. There are two substrates suitable for $Ga_{1-x}In_xSb$ epitaxy - GaSb and InSb. We chose the $Ga_{1-x}In_xSb$/GaSb approach because this allows both epitaxial step and linear grading to be used while in the $Ga_{1-x}In_xSb$/InsB system only linear grading can be used since the lattice constant of the epitaxial deposit is smaller than that of the substrate.

The (111)B direction was chosen as the primary growth direction for the seeds since their intended future use is for a bulk growth techique and historically the best bulk growth of III-V compounds has been accomplished using that direction.

Initially LPE growth attempts were made using the linear compositional grading technique because it is experimentally simpler than the

STEP GRADED

- LATTICE MISMATCH BETWEEN EPITAXIAL LAYER AND SUBSTRATE GENERATES INITIAL MISFIT DISLOCATIONS.
- IDEALLY MISFIT DISLOCATIONS "THREAD IN AND OUT" AT COMPOSITIONAL INTERFACES.
- NO OTHER MISFIT DISLOCATIONS NEEDED AT SUBSEQUENT ABRUPT COMPOSITIONAL STEPS.

LINEAR GRADED

- INCLINED DISLOCATIONS PROPAGATE TO ACTIVE MATERIAL.
- DISLOCATION DENSITY PROPORTIONAL TO COMPOSITION GRADIENT.

Fig. 5 Epitaxial growth techniques for lattice mismatched systems.

step grading technique. Two techniques were attempted, first the gradual lowering of the Ga-In-Sb liquid temperature which should, because of the phase diagram, increase the X value in the epitaxial deposit. Second, the periodic addition of small amounts of In to the Ga-In-Sb melt which should have the same effect. However, neither technique produced X values beyond the X value known to be in equilibrium with the initial liquid. This is due to an effect called lattice "latching" or "pulling" once a certain lattice constant, or X value, is established, the epitaxial deposit continues to grow at that lattice constant despite the fact that the composition of the liquid is changed such that the lattice constant should increase. We have also observed this effect in the $InAs_{1-x}Sb_x$ system. Unable to increase the In fraction with the linear grading technique we redirected the growth attempts to the compositional step grading technique. Using growth parameters established for relatively smooth $Ga_{1-x}In_xSb$ epitaxial growth for the (100) orientation established in other programs, resulted in epitaxial deposits with excessive "hillock" formation for (111) orientation. This is shown for a single $Ga_{.90}In_{.10}Sb$ layer on (111)B GaSb in Fig. 6. Shown is the entire wafer, general surface morphology and the top of a hillock under higher magnification. The "slash" at he top of the hillock appears to be a facet formation and is always parallel to a <110> direction. The general "roughness" of the epitaxial layer is due to the lattice mismatch. Height differences, taken from cleaved and stained cross-sections between valleys and tops of hillocks are typical 10 - 20 μm which is undesirable since it would lead to a nonplanar growth front in the bulk growth experiments which would follow. This is shown in Fig. 7. The origin of these "hillocks" is unknown, but have been observed in other III-V solid solution growth.

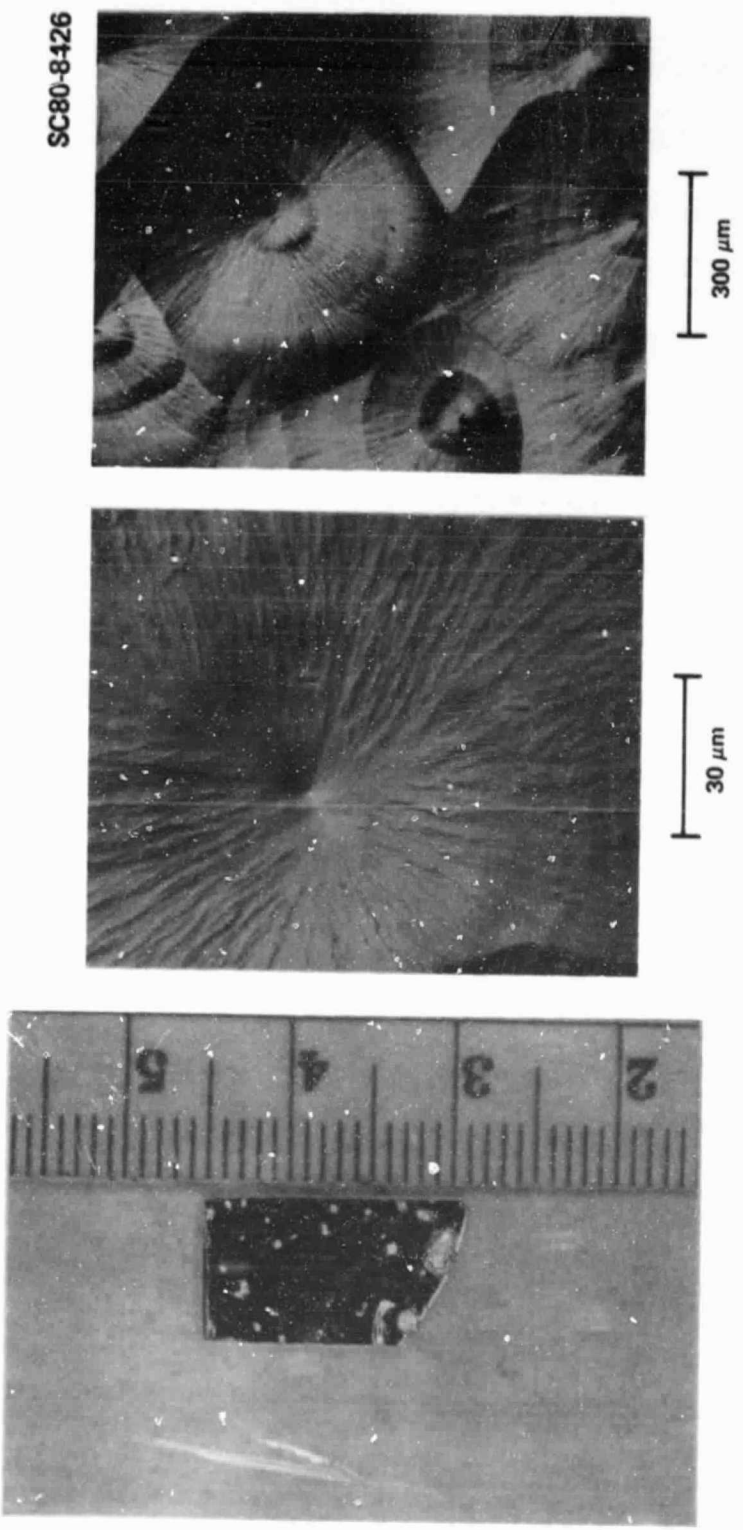

Fig. 6 Wafer, surface morphology showing "Hillock" formation on (111)B LPE grown $Ga_{.90}In_{.10}Sb$.

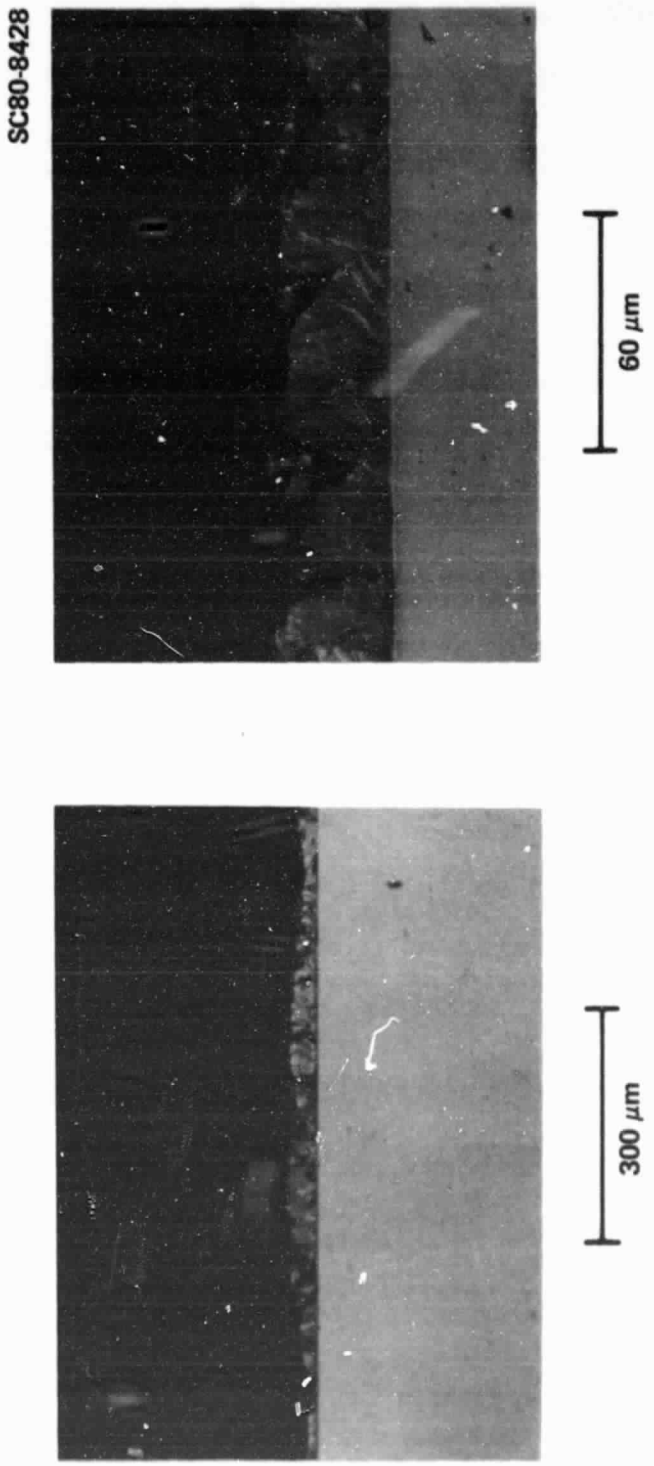

Fig. 7 Cross-section of LPE grown $Ga_{.90}In_{.10}Sb$.

Raising the temperature above 500°C eliminated the hillock formation. The surface morphology of a typical single $Ga_{.90}In_{.10}Sb$ layer grown on GaSb is shown in Fig. 8a. While there is no "hillock" formation, the rough surface morphology is partially a result of the lattice mismatch between the $Ga_{.90}In_{.10}Sb$ epitaxial layer and the GaSb substrate.

In Fig. 8b, the etch pit density (E.P.D.), as revealed by chemical dislocation etching, is shown for a $Ga_{.90}In_{.10}Sb$ layer grown directly on GaSb. The E.P.D. is approximately 10^6 cm^{-2} which is reasonable for the lattice mismatch involved. The dislocation distribution, however, is not uniform but tends to "cluster." The majority of the dislocations are found along lines parallel to <10> directions. This is seen clearly in the center of Fig. 8b. The reason for this "clustering" is not known at present.

Another reason for the surface roughness of the $Ga_{.90}In_{.10}Sb$/GaSb structure may be compositional variations in the epitaxial layer caused by convection in the liquid during growth. X-ray topography studies of the $Ga_{.90}In_{.10}Sb$ material are shown in Fig. 9a and b.

Figure 9a is a topograph of the as-grown material. To ensure that surface morphology of the $Ga_{.90}In_{.10}Sb$ material did not contribute to the structure seen in Fig. 9a, the material was polished and again analyzed by x-ray topography. The result is shown in Fig. 9b. There is virtually no difference between the features of Fig. 9a and 9b. The conclusion that can be drawn from the x-ray topographs is that the $Ga_{.90}In_{.10}Sb$ material is not single, but polycrystalline.

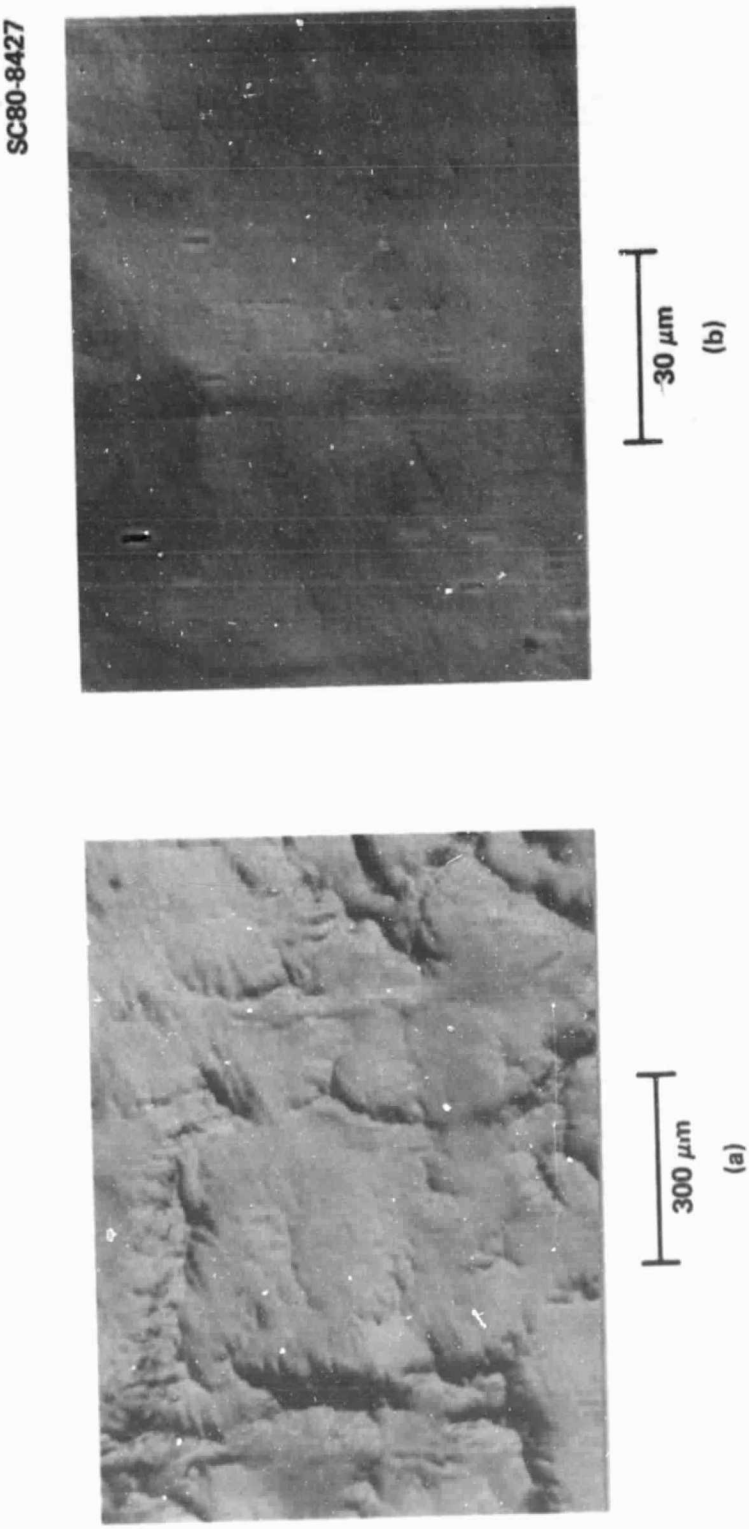

Fig. 8 Morphology and etch pit density of LPE grown (111)B $Ga_{.90}In_{.10}Sb$.

Fig. 9 X-ray topograph of (111)B $Ga_{.90}In_{.10}Sb$ epitaxial layer.
a) As grown
b) Polished

To eliminate the GaSb substrate quality as a potential source of this polycrystallinity in the epitaxial layer, a x-ray topograph was taken of a polished (III)B GaSb substrate. The result is shown in Fig. 10. The topograph is basically featureless, indicating single crystal material. The variation in intensity across the slice is due to slight bowing of the wafer due to polishing. The fine dark lines visible in some parts are scratches on the photographic film from which the print was taken and not features of the GaSb substrate material. The dark line running across the center of the wafer is probably due to overexposure because of mechanical hangup of the translation at that position during exposure.

From the above results it became obvious that in order to achieve higher quality epitaxial $Ga_{1-x}In_xSb$ material smaller compositonal steps than 10% were needed. However, numerous attempts to use a large number of compositional steps met with very little success. Typically, using multiple layers resulted in higher quality material, that is lower etch pit density but rather poor morphology. This is shown in Fig. 11 where the cross-section and morphology for a two and four layer structure are compared. This is for (100) structures grown under a separately funded program. While the four layer structure has a much lower EPD than the two layer structure its morphology is much rougher. The same effects occurred for (111) growth except for even rougher morphology with very little useful material due to numerous melt spots. These results are remarkably different from those found for the $InAs_{1-x}Sb_x$ system where the use of multilayers not only reduced the EPD but also improved the surface morphology.[5] Possible explanation of this effect in the $Ga_{1-x}In_xSb$ system is that the solid and liquid are of comparable density

SC80-8429

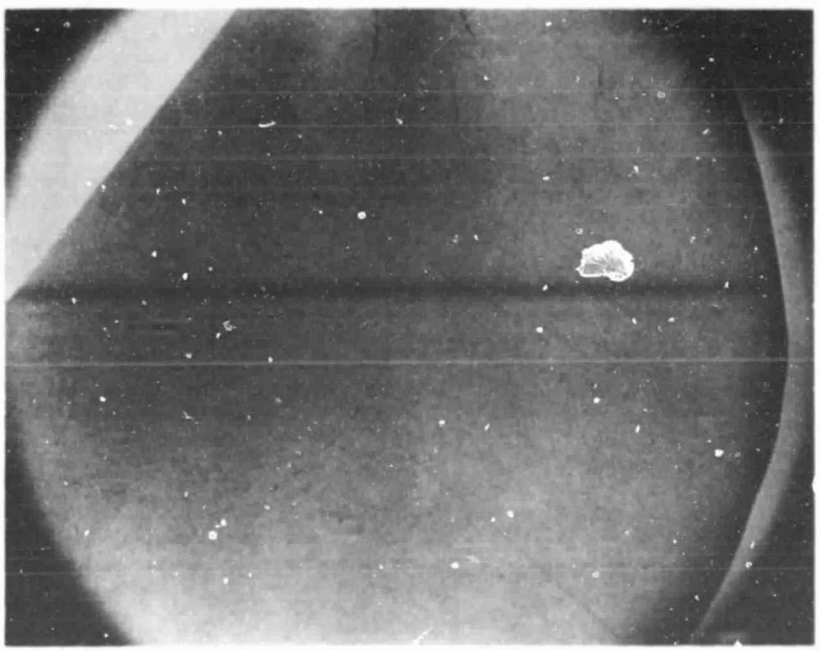

Fig. 10 X-ray topograph of (111)B GaSb substrate.

SC80-8971

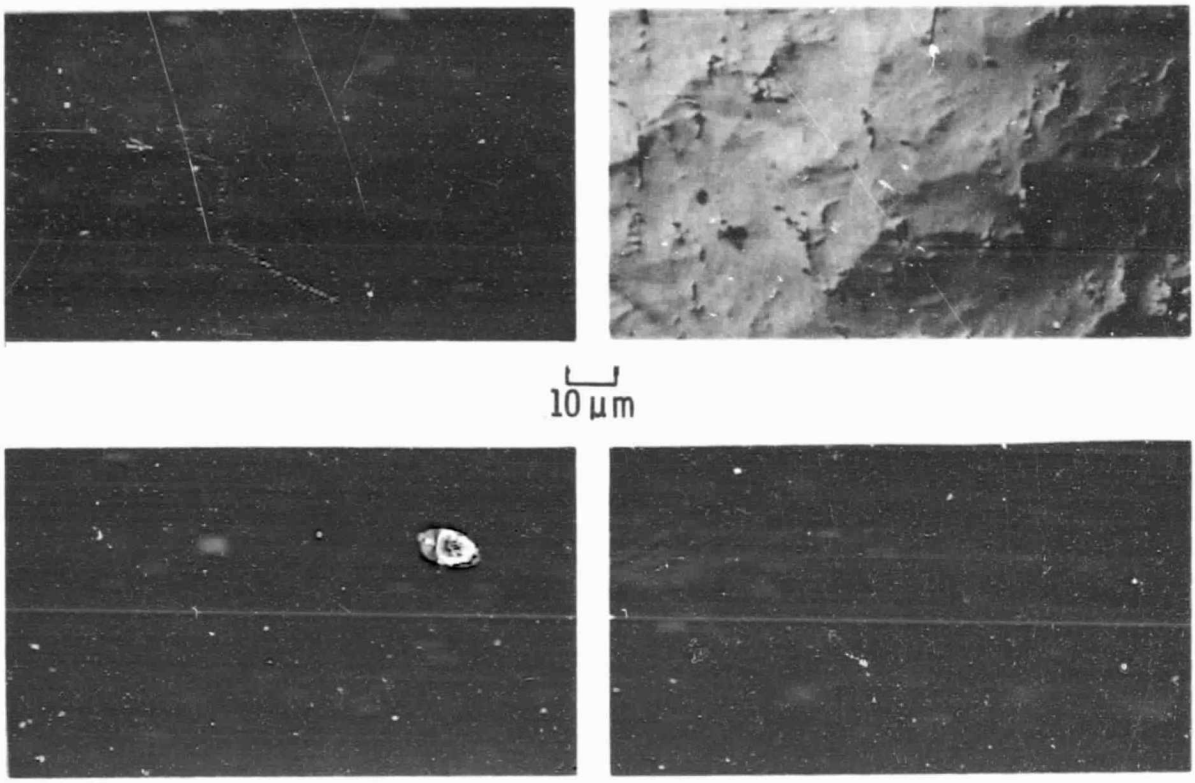

Fig. 11 Cross-section and morphology of a two and four multilayer (100) LPE grown $Ga_{1-x}In_xSb$ structure.

and that during the repeated mechanical sliding of the melts on and off the substrate excess solid is "rolled" into the growth interface. Poor epitaxial growth occurs at and around these particles, typically resulting in metallic inclusions and melt spots.

In view of these difficulties with the LPE multilayer step grading and linear grading approach, on both this and other programs, we began to consider vapor epitaxial approaches.

2.2 Vapor Phase Epitaxy of $Ga_{1-x}In_xSb$

The advantages of vapor phase epitaxy (VPE) over liquid phase epitaxy lie in several areas. First, there is better control over compositional grading both step or linear since changes in vapor composition are readily accomplished allowing both a larger number of multilayers to be used or very smooth linear grading to be achieved since the effect of lattice pulling is not as prominant in vapor epitaxy. Second, thickness control in VPE is superior to LPE which is important for a lattice mismatched system where a large number of thin compositional graded layers is desirable to reduce the EPD. Third, in VPE no thermodynamic limitations exist between liquid and substrate allowing epitaxy in a system were no equilibrium exist between liquid and substrate. This consideration does not apply to this program but was important for other programs.

With IR&D funds a prototype VPE system was assembled. The organometallic approach was used because of the low vapor pressure of elemental antimony makes the chloride transport technique unattractive. The flow

diagram of the system is shown in Fig. 12. High purity hydrogen controlled by mass flow controllers are bubbled through the metal alkyls of trimethylgallium (TMGa), triethylindium (TEIn), and trimethylantimony (TMSb). This gas mixture is further diluted by hydrogen carrier gas, fed into a bell jar where the organo metallics are thermally decomposed forming $Ga_{1-x}In_xSb$.

Initial)0) growth results, funded by IR&D and other programs, were promising. First achieved X values of up to .6 in relatively smooth layers. The highe X value achieved for a reasonably smooth layer by LPE techniques (111) (100), has been x = 0.3. Furthermore, for the first time we observed "cro atch" in epitaxial $Ga_{1-x}In_xSb$ a phenomena never observed in LPE grown mat l. Cross-hatch is usually a sign of higher quality material because is the result of an "ordered" set of misfit dislocation generated by la -mismatch. Results are shown in Fig. 13. The linear graded (100) material, mplished manually, shows a smooth morphology even at high X values. On the s of these results a second generator OM-VPE reactor was built where all flows are under computer control. Figure 14 is an X-ray topograph of a $Ga_{.92}In_{.08}Sb$ step graded layer grown on (100) GaSb. The seven compositional steps consist of 1% In fraction increments, each layer is .5 μm thick; the final constant composition layer is 3.6 μm thick. Of note is the regular cross-hatch pattern indicating that most of the misfit dislocations are confined to the compositional buffer layer interfaces resulting in a final constant composition layer with a low dislocation density - a result confirmed by chemical dislocation etching. However, using growth parameters developed for (100) growth for (111) growth for this program resulted in basically polycrystalline material. Figure 15 is a comparison between a concurrent

ORIGINAL PAGE IS
OF POOR QUALITY

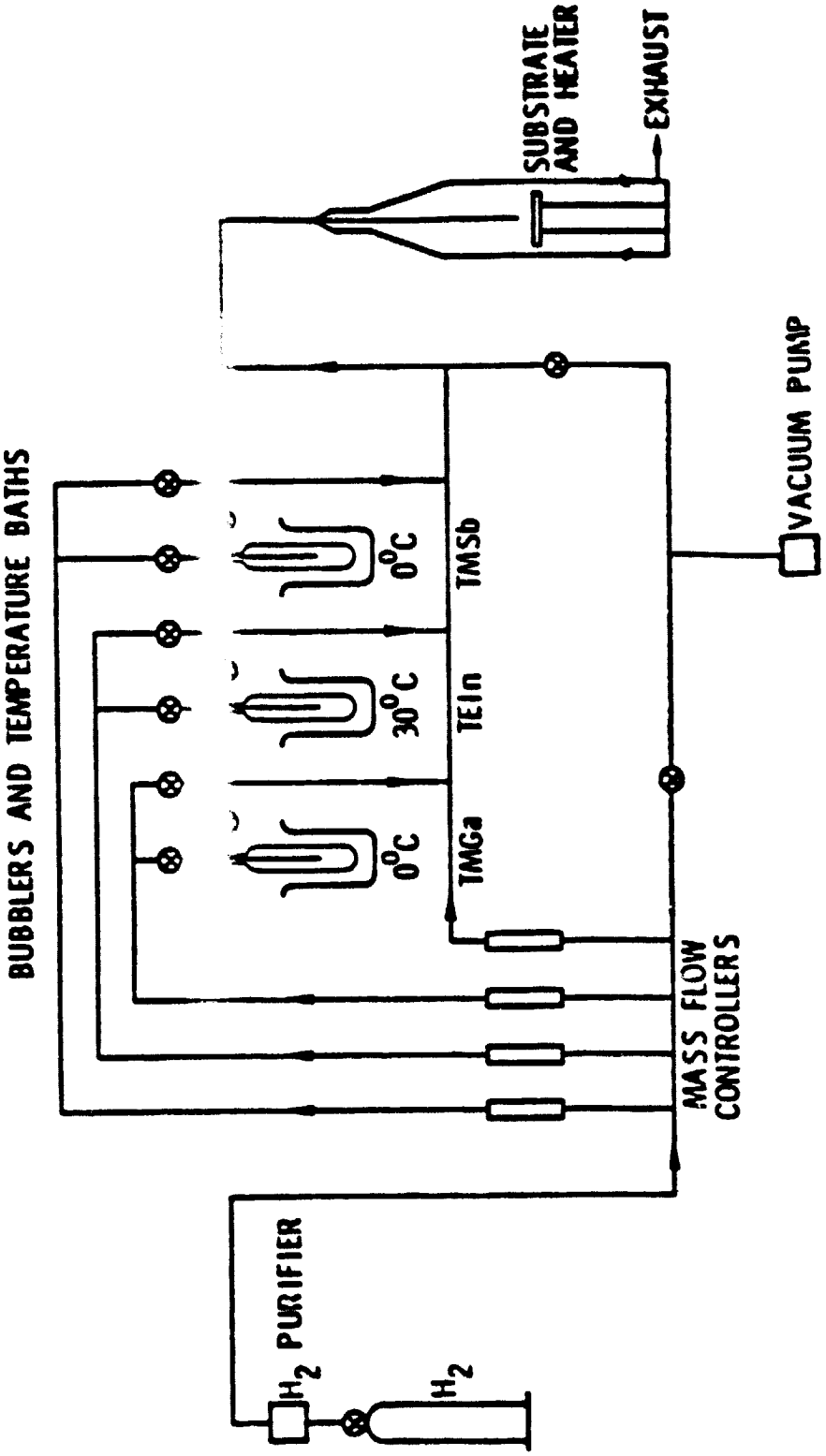

Fig. 12 Simplified VPE flow diagram.

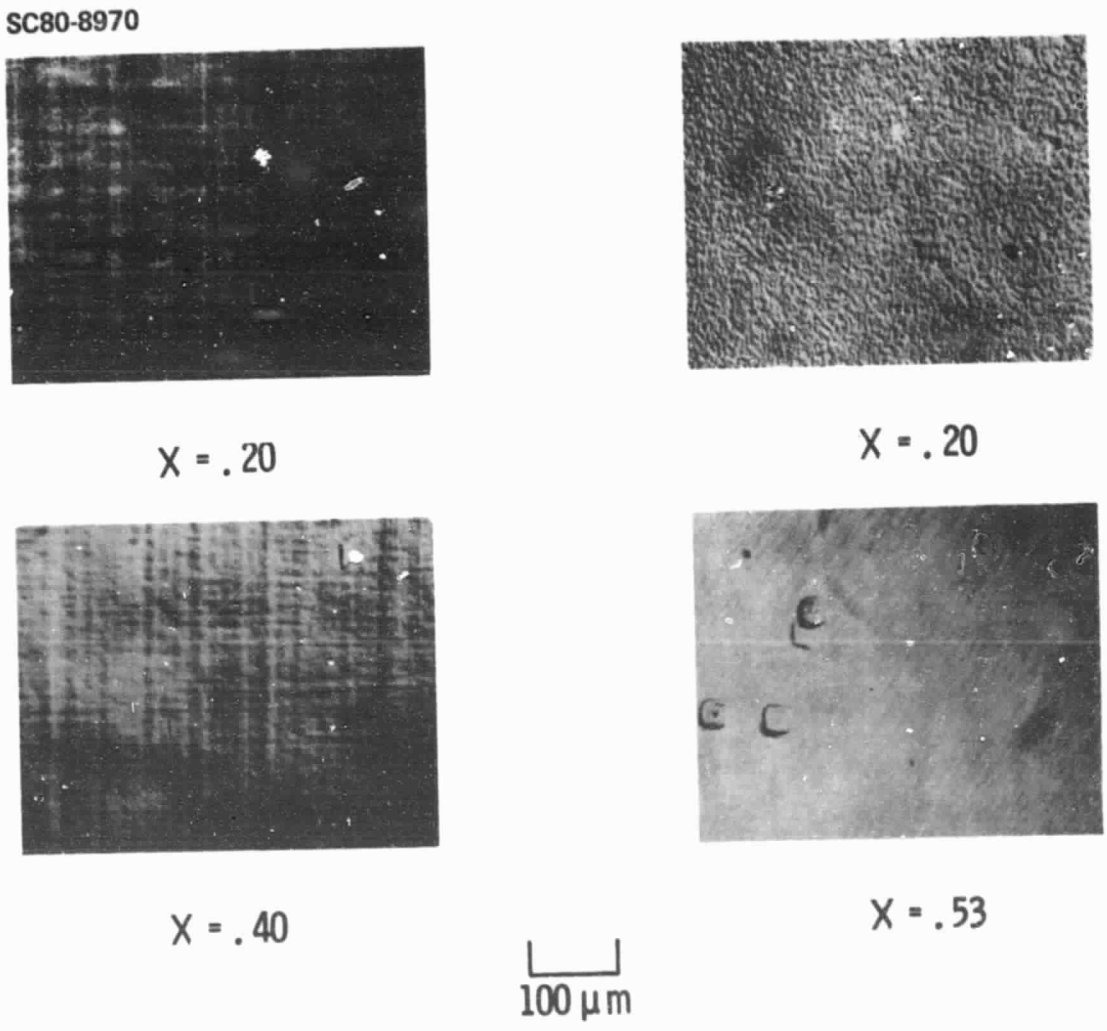

Fig. 13 Comparison of surface morphologies of graded and nongraded OM-VPE (100) $Ga_{1-x}In_xSb/GaSb$.

SC80-8969

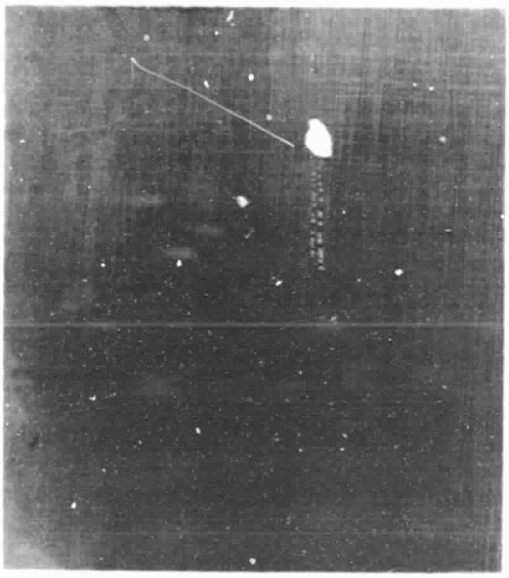

Fig. 14 X-ray topograph of an OM-VPE grown, step graded (100) $Ga_{.92}In_{.08}Sb/GaSb$ structure.

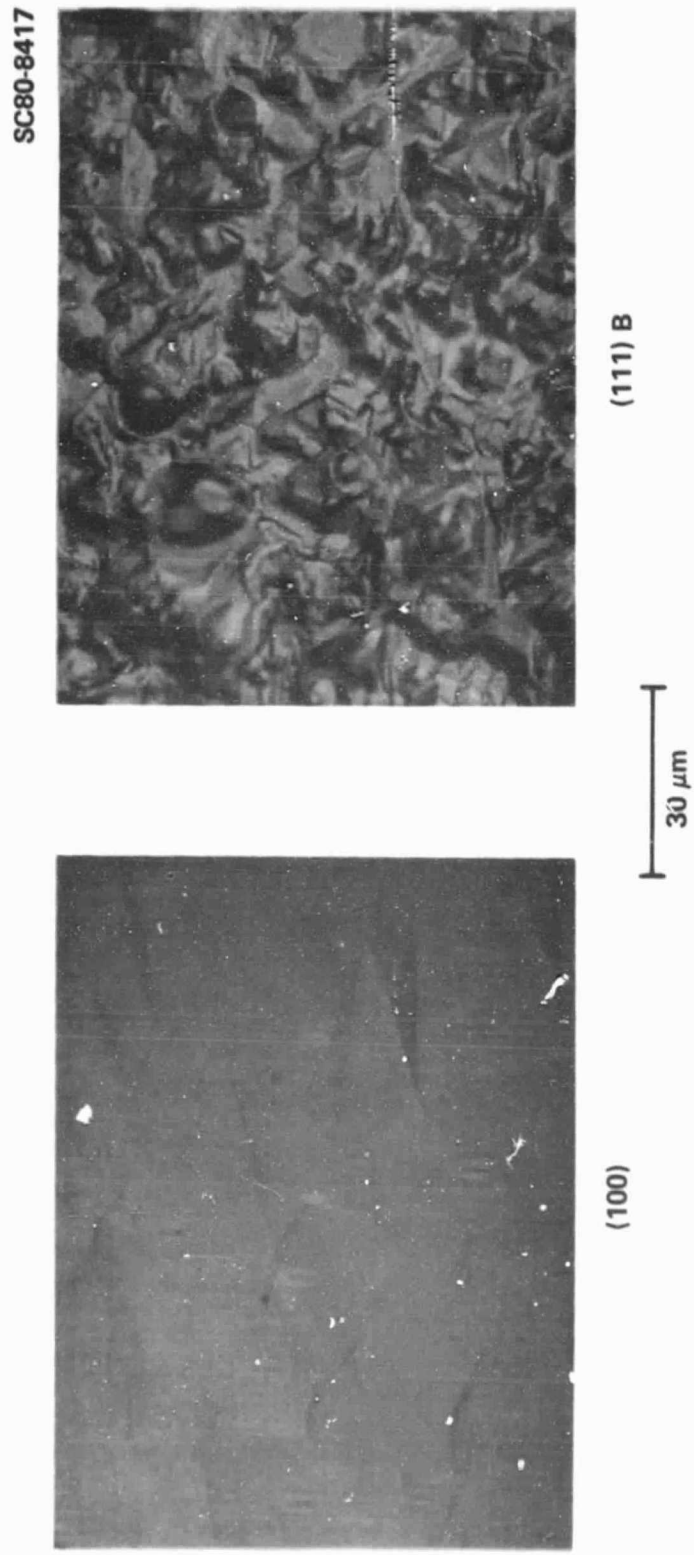

Fig. 15 Comparison of (100) and (111)B OM-VPE grown $Ga_{.90}In_{.10}Sb$.

(100) and (111)B $Ga_{.90}In_{.10}Sb$ growth. While the (100) growth is relatively smooth, the (111) growth is polycrystalline. Changing growth conditions from optimum (100) parameters resulted in no improvement for (111) growth. These results, plus other developments led to reassessment of the proposed approach which is discussed in the next section.

2.3 Assessment and Conclusion (Original Approach)

The difficulties encountered both with the LPE and OM-VPE techniques in the growth of bulk $Ga_{1-x}In_xSb$ will make the seed synthesis for the space experiments a major task, but it is a task that can be solved especially in view of the recent advances in MBE and OM-VPE technology. Ironically, success in growing high quality lattice-mismatched III-V structures by those techniques would reduce the need for III-V solid-solution bulk cyrstals for the realization of lattice matched device structures. Furthermore, we believe that quaternary epitaxial growth on existing binary compound substrates will solve most of the III-V device structure requirements. Quaternary growth allows a decoupling of the lattice constant and energy gap allowing lattice matched heterostructures with varying bandgap to be grown. At the time the proposal for this project was written many of the problems that hindered development of several quaterraries because of thermodynamic instability (AlGaAsSb on InP for example) between substrate and liquid in LPE no longer apply since MBE and OM-VPE techniques have matured. Neither of these techniques has the thermodynamic limitations of the LPE approach. The only region in which quaternaries can not be grown is in the IR region since no intermediate substrate exist between the end points of InAs, GaSb and InSb. (see Fig. 1). But even

in this range, for IR applications, the superior performance of $Hg_{1-x}Cd_xTe$ IR devices will relegate III-V IR detectors to a secondary backup status.

The significance of the above observations is that growth of bulk III-V solid solutions single crystals in a low gravity environment will not have a major technological impact and in view of this the research effort was changed into an area where low gravity growth would have a potential major technological impact - the bulk growth of CdTe.

3.0 ALTERNATE APPROACH

3.1 Material Selection

CdTe was selected as a candidate for low gravity growth because of critical needs for large, high quality single crystals in several areas. First and foremost is the need for larger area, high quality CdTe single crystal substrates for $Hg_{1-x}Cd_xTe$ backside illuminated IR focal planes. Currently, $Hg_{1-x}Cd_xTe$ epitaxy is limited by the grain size of commercially available Bridgeman grown multigrain ingots. Other fields which would benefit from the availability of large single crystals of CdTe are the optical modulators and X-ray detector areas.

Other considerations which led to the selection of CdTe is that it is a binary hence there is no separation of liquidus and solidus thereby easing the necessity for a large temperature gradient across the liquid-solid interface to maintain interface stability required for ternary, such as $Ga_{1-x}In_xSb$ growth. Also, with the CdTe approach there is no delay due to seed generation - commercial multigrain ingots typically contain grains large enough to serve as seeds for immediate start or normal gravity float zone experiments.

A further advantage of the current material approach is that it addresses NASA needs in the IR detection area. $Hg_{1-x}Cd_xTe$ will dominate the IR field due to ease of wavelength tunability. HgTe-CdTe are nearly lattice matched and high performance IR detectors have been fabricated in LPE grown $Hg_{1-x}Cd_xTe$/CdTe structures with X values varying from x = .40 to x = .20. This corresponds to the 1 - 12 μm IR region. In contrast, a previous longer

term effort to achiev a similar tunability in the $InAs_{1-x}Sb_x$ system failed because of the probl s associated with lattice mismatch.

Last, the n approach will benefit from "spillover" support from other major DoD fund CdTe and HgCdTe programs.

Currently p ied growth techniques at the Science Center are the Bridgman technique a closed tube vapor transport. The Bridgman technique will be developed tc process where high crystallinity multi grain ingots are routinely grown to s y near term substrate needs for $Hg_{1-x}Cd_xTe$ epitaxial processes. For larg single crystals of CdTe we are developing a closed tube vapor transport chnique whose feasibility was recently demonstrated by growing a small eigh ^{3} single crystal.

3.2 Rationale

Why use th oat zone technique in a low gravity environment for CdTe? Because that hnique has inherently the best thermal symmetry of all the major growth tec ques which can result in the synthesis of very large crystals. In other k growth techniques such as Bridgman and Czochralski the thermal environment changes as the liquid fraction decreases and the solid fraction increases, especially if the thermal conductivities of the liquid and solid differ widely. This limits the size of the crystal that can be grown since compromises need to be made between the optimum thermal environment for the start and end of the growth. No such compromises need to be made for the float zone technique because it has a high degree of thermal symmetry because of its physical configuration which keeps the mass ratio of the liquid to

solid constant during growth. Furthermore, float zoning utilizes all of the advantages that low gravity offers - attributes that other growth techniques such as Czochralski and Bridgman do not.

The need for low gravity arises because density and surface tension consideration for CdTe will probably limit any float zoning to very small diameter crystals in a normal gravity environment. An estimate of zone size is made in Section 3.3.

3.3 Technical Problem

The synthesis of completely single crystal CdTe has not yet been achieved despite the usage of a variety of techniques. A typical multigrain, vertical Bridgman grown CdTe crystal is shown in Fig. 16. The grain boundaries are enhanced by a felt tipped pen. The use of other techniques such as traveling zone,[6] traveling solvent,[7] Czochralski,[8] solution growth[9] and solvent evaporation[10] have had similar results. While no investigator has been able to identify the underlying cause or causes that result in this multigrain growth behavior several areas which are important in the growth of CdTe have been identified. But before covering these areas, the physical properties involved in the preparation and crystal growth of CdTe are discussed.

Bulk CdTe crystalizes in the zinc-blende structure with a lattice constant of 6.48 Å, and possesses a relatively low thermal conductivity of 0.06 watts/cm K. The thermal expansion coefficient is 5.2×10^{-6} C^{-1}.

SC79-6136

Fig. 16 Commercial Bridgman grown CdTe boule.

The CdTe temperature vs composition projection of the phase diagram[11] is shown in Fig. 17a. The maximum melting point is 1092°C and lies slightly on the Te-rich side. The homogeneity region of CdTe, represented by a solid line in Fig. 17a, extends both into Te- and Cd-rich sides from the stoichiometric composition. Deviation from the stoichiometric composition determines the conduction type and carrier concentration of the material in the absence of impurity doping. Cd and Te saturated CdTe have n- and p-type conduction, respectively, with the carrier concentration proportional to the deviation from stoichiometry. Compositions near stoichiometry are high resistivity to semi-insulating. Shown in Fig. 17b is a greatly expanded schematic of the homogeneity range of CdTe.[12] The border of this homogeneity range, however, is not only influenced by the liquid composition, but also by the vapor composition over liquid and solid. The temperature vs pressure projection of the Cd-Te phase diagram is shown in Fig. 18.[13] At points along the loops marked p_{Cd} and p_{Te_2} solid, liquid and vapor co-exist. Inside the loop, only solid and vapor exist; and only liquid and vapor in the region outside the loops. The dashed line for each loop is the vapor pressure of p_{Cd} and P_{Te_2}, at the homogeneity limit, over Te saturated CdTe, while the solid line for each loop is the vapor pressure of p_{Cd} and p_{Te_2} over Cd saturated CdTe. The maximum melting point of CdTe lies where the dashed and solid lines meet. p^o_{Cd} and $p^o_{Te_2}$ are the vapor pressures of pure Cd and Te_2, respectively. At any temperature, the lowest total pressure exists for congruently subliming CdTe satisfying the condition

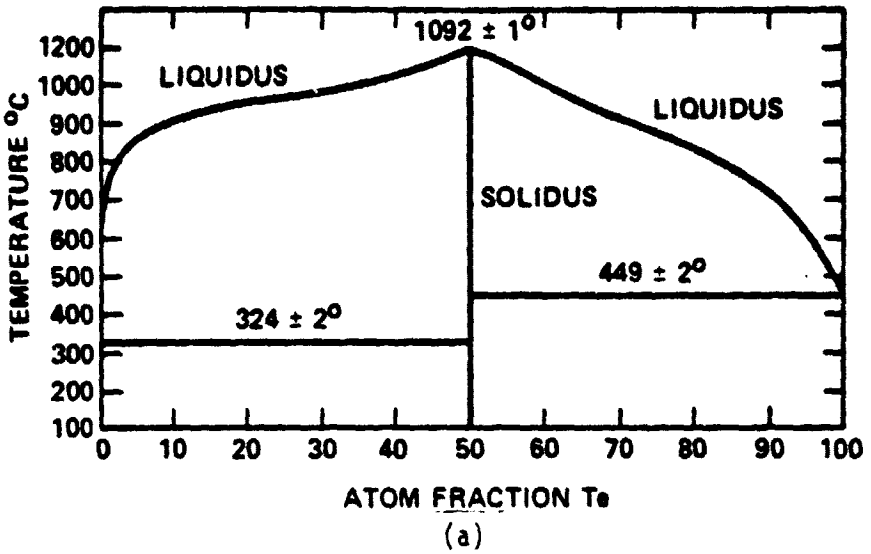

(a)

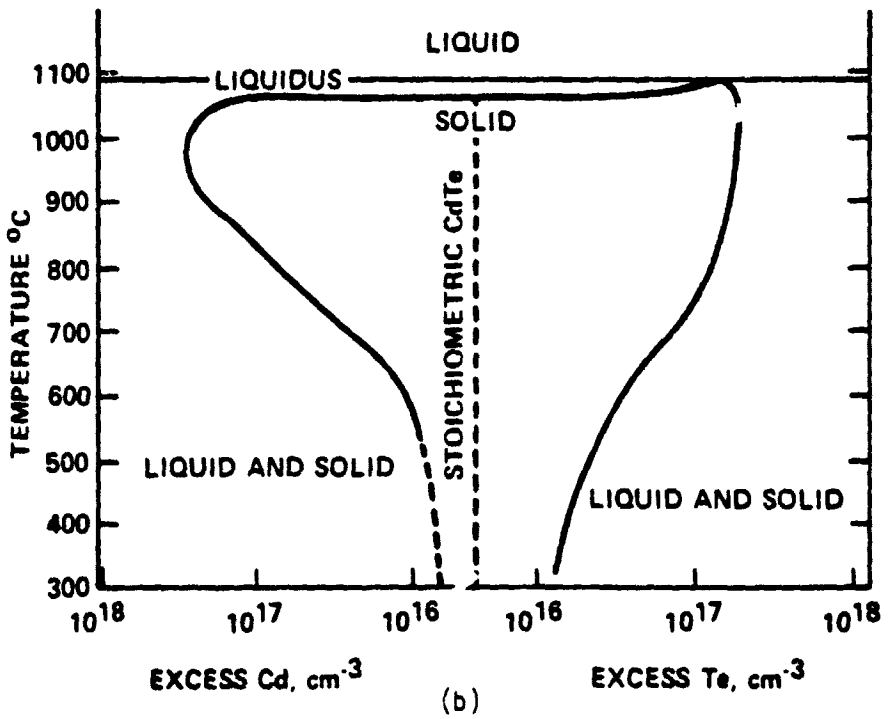

(b)

Fig. 17 Cd-Te phase diagram
a) Temperature vs composition projection.
b) Homogeneity region of solid CdTe.

SC79-5605A

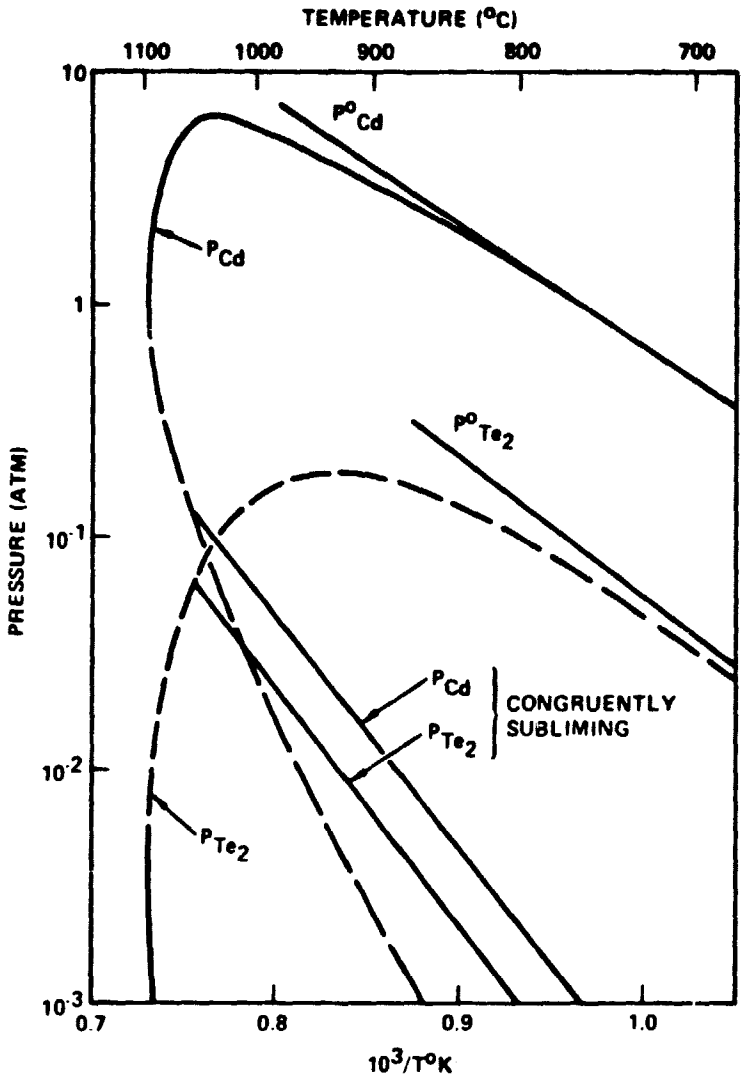

Fig. 18 CdTe phase diagram pressure vs temperature projection.

$$P_{Cd} = 2P_{Te_2}$$

Experimentally Cd (atoms) and Te_2 (molecules) are the only constituents found in the vapor phase over CdTe.[14,15] At the maximum melting point of CdTe, the vapor pressure for p_{Cd} and p_{Te_2} are 0.65 atm and 5.5×10^{-3} atm for Cd and Te_2 saturated CdTe, respectively. For congruently subliming CdTe, the total vapor pressure is approximately 0.18 atm at the melting point.

This brings up the first area that must be addressed during the crystal growth of CdTe - the loss of Cd. Stoichiometric growth conditions must be maintained via control of the gas phase over the liquid. This is relatively simple with a closed ampoule configuration such as Bridgman or traveling zone but more difficult with float zoning because Cd will condense on any cold surface. This can be prevented by having a hot wall system where all surfaces are at such a temperature that the Cd pressure equals that of Cd over liquid CdTe. Additionally, from Fig. 18 we can see that a Cd reservoir at ≈ 720°C will establish a Cd pressure equal to that of Cd over liquid CdTe thus establishing equilibrium conditions. Care must be taken to accurately control the temperature and the pressure because too low a Cd pressure in the container will lead to a loss of Cd from the molten zone while too high a Cd pressure will cause the zone to become Cd-rich - i.e., both conditions will lead to nonstoichiometric growth conditions.

Fast growth rates were not expected for CdTe because of its rather poor thermal conductivity which limits the temperature gradient that can be established at the liquid-solid interface.

The near term objectives of the revised program were as follows:

Task I -Perform initial floating zone growth of CdTe using existing equipment.

Task II -Prepare a preliminary design for a second generation floating zone apparatus, using data from Task I.

Task III -Perform ground-based (normal gravity) experiments in support of low-gravity (space) floating zone growth of CdTe.

4.0 EXPERIMENTAL APPROACH

What zone length can be expected for CdTe? Using Heywang's[2] criteria for the maximum zone length possible in a normal gravity environment

$$\ell_m \sim 2.8 \quad \frac{\gamma}{\rho g}$$

where

γ = surface tension

ρ = density

g = gravitational constant

for the CdTe case we had to assume a value for the surface tension since no data could be found

CdTe

γ = 200 dynes/cm

ρ = 5.86 gram/cm^3

$\ell_m \sim 0.5$ cm

and for comparison Si

Si

γ = 700 dynes/cm

ρ = 2.53 gram/cm^3

ℓ_m ~ 1.5 cm.

Thus for CdTe, because of lower surface tension and higher density, the zone length is three times shorter than for Si which can be float zoned in normal gravity. Therefore the initial experiments were traveling zone growth where the liquid zone is supported by an ampule wall. These experiments were designed to optimize growth and equipment parameters for the float zone experiments.

To achieve the smallest possible molten zone, RF heating was used. Since the manual control of the Lepel RF generator was insufficient to ensure zone stability the RF generator was modified to accept and respond to an 0 - 5 mV DC control signal from a commercial (Research Incorporated) temperature controller. Both temperature control via a thermocouple feedback loop or manual control RF power output were possible. Growth experiments were carried out using manual control of the 0 - 5 mV DC signal since initial experiments using the temperature control mode via a thermocouple feedback look resulted in large temperature fluctuations. This was not unexpected since spurious temperature fluctuation were intruduced due to convective air currents around the ampule to which the thermocouple and controller responded. These problems were avoided by using the RF generator in an essentially manual mode through

manual control of the 0 - 5 mV DC signal of the R&I controller which allowed reproducible RF power levels to be established.

Growth attempts were carried out in closed quartz ampules of six to fifteen mm diameter. The apparatus in which the experiments were carried out is shown during operation in Fig. 19 and is essentially a linear drive mechanism that allowed smooth ampoule motion to occur at preselected rates.

SC81-14032

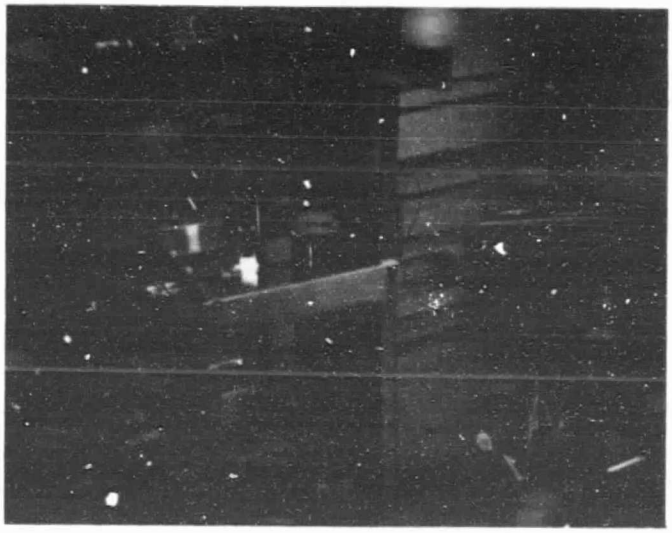

Fig. 19 Linear motion apparatus for CdTe float zone experiments.

5.0 EXPERIMENTAL RESULTS

Initial CdTe growth experiments were carried out using the t lling zone technique where the liquid zone is supported by the ampoule wall establish growth parameters for the floating zone growth experiments. During this phase, two problem areas arose and caused considerable delay in achieving several planned milestones. These problem areas consisted in first, the ampule and CdTe chage preparation and second, the establishment of a stable liquid CdTe zone. Following is a detailed discussion of the problem areas attempted solutions and their results.

5.1 Ampule and CdTe Preparation

The three major methods used to prepare the quartz ampule with the CdTe charge for the traveling zone experiments are listed in Table 1. The initial attempt of preparing a charge for the traveling zone experiments consisted of filling a 6 or 12 diameter clean quartz ampoule with crushed CdTe material which was typically obtained from Bridgman grown ingots. The charge was compacted as much as possible by mechanical vibration using an ultrasonic cleaner. A quartz sealing cup was then placed directly behind the charge. After evacuating into the low 10^{-6} torr range the ampoule was then sealed off at the sealing cup by fusing the ampoule wall against the sealing cup with the use of a hand torch. Next, after securing the ampoule in the float zone apparatus, a liquid zone was established via RF heating (Section 5.2). However, traveling zone experiments conducted with ampoules prepared in the above

Table 1 Sample preparation

TECHNIQUE	RESULT
CRUSHED CdTe MATERIAL	SEVERE VAPOR TRANSPORT SEPARATION BETWEEN LIQUID AND SOLID
PREMELTING CRUSHED CdTe MATERIAL	NON STOICHIOMETRIC MIXTURE AMPULE BREAKAGE
RECAST CdTe ROD PLUS THIN CRUSHED CdTe POWDER ON PERIMETER	ALLOWED ≃ 2 cm OF GROWTH PRIOR TO COMPLETE LIQUID SOLID SEPARATION

described manner failed due to an unexpected problem - the severe vapor transport of CdTe from the liquid zone to colder ports of the ampoule. Some Cd loss had been expected but not the large scale loss of CdTe which rapidly led to a physical separation between solid and liquid. Various attempts were made to eliminate this separation by reducing the vapor transport. Using finely crushed CdTe powder to achieve a higher fill factor plus backfilling the ampoule with argon or hydrogen gas were successful only in that the time before physical separation between liquid and solid occurred increased.

The next attempt to obtain a high fill factor in the ampoule to prevent vapor transport consisted of premelting the entire charge using a long Inconel sleave heated by RF power to above the melting point of CdTe. Melting the entire charge initially reduced vapor transport in subsequent travelling zone experiment but typically resulted in nonstoichiometric CdTe charges due to volatilization and transport of the higher vapor pressure Cd species. In addition, with this charge preparation ampoule breakage would often occur because of "wetting" of the quartz by the CdTe material. Ampule breakage occurred both on cool down after the premelting cycle or in the subsequent reheating in the traveling zone experiments. Coating the ampoule with a thin pyrolytic carbon coating to prevent "wetting" and also to allow for thermal expansion was effective only in preventing ampoule breakage upon cooldown from the premelting cycle. Upon heating the partially destroyed graphite coating typically could not prevent ampoule breakage.

The final and most successful charge preparation consisted of the following rocedure. A CdTe rod was prepared by first melting crushed CdTe

(contained in a quartz ampoule) in a tubular, resistively heated furnace. After soaking the CdTe charge above the melting point for several hours to ensure homogenization, the furnace temperature was then lowered at the rate of approximately 50°C/hour causing the CdTe to solidify in a highly polycrystalline state. The precast rod was then inserted in a quartz ampoule (coated with pyrolytic graphite) selected for a loose fit in order to prevent ampoule breakage upon heating. The gap between the ampoule wall and the CdTe rod was filled with finely crushed CeTe material which was compacted as much as possible by mechanical and ultrasonic vibrations. Upon evacuating and partial backfill with H_2 gas this charge was then sealed off. This charge preparation virtually eliminated ampoule breakage and allowed 2-5 cm of growth to occur prior to liquid-solid separation. In addition CdTe charges prepared in this manner were reasonably stoichiometric and thus close to the maximum melting point of CdTe.

5.2 Zone Melting of CdTe

Successful crystal growth by zone melting techniques depend critically on the stability of the molten zone. In this program considerable effort was spent on the development of a heating technique that would result in a uniform, stable molten CdTe zone. RF heating was selected as the basic heating approach since large amounts of power can be concentrated over small areas and volumes.

Initial CdTe zone melting experiments were of the indirect heating nature - a graphite susceptor, heated by RF power, melted the CdTe. This is

the simplest approach possible in heating CdTe since solid CdTe will not couple to RF power because of its low conductivity. A schematic of the technique is shown in Fig. 20.

Since direct coupling between the RF powe and solid CdTe is not sufficient to melt the CdTe, a graphite suceptor was inserted between the ampoule containing the CdTe charge and the RF coil. In this case, the graphite couples efficiently with the RF and the CdTe is melted by radiative heating by the hot graphite. The hot graphite, however, must be protected from the air ambient since oxidation and rapid disintegration will occur. The apparatus shown in Fig. 20 was designed and constructed to provide an inert gas ambient for the graphite. The apparatus consists of an outer quartz sleeve and an inner quartz susceptor carrier. The susceptor is a graphite ring bracketed by two alumina refractory rings designed to prevent radiative heat end losses. Initial attempts to liquify CeTe were not successful - vaporization of the CdTe would occur prior to melting because of the low thermal conductivity of CdTe and the re vely coarse CdTe pieces. Crushing the CdTe to a fine powder, average size approximately two-to-three mm, plus backfilling the ampoule with a partial atmosphere of hy an excellent heat conductor, enabled us to melt the CdTe successfully (see Section 5.1 for CdTe charge preparation).

However, after several zone melting experiments it became apparent that this heating approach entailed several disadvantages. First, the hot graphite needed protection from the air ambient because oxidation lead to rapid degradation of the susceptor. The arrangement used to protect the

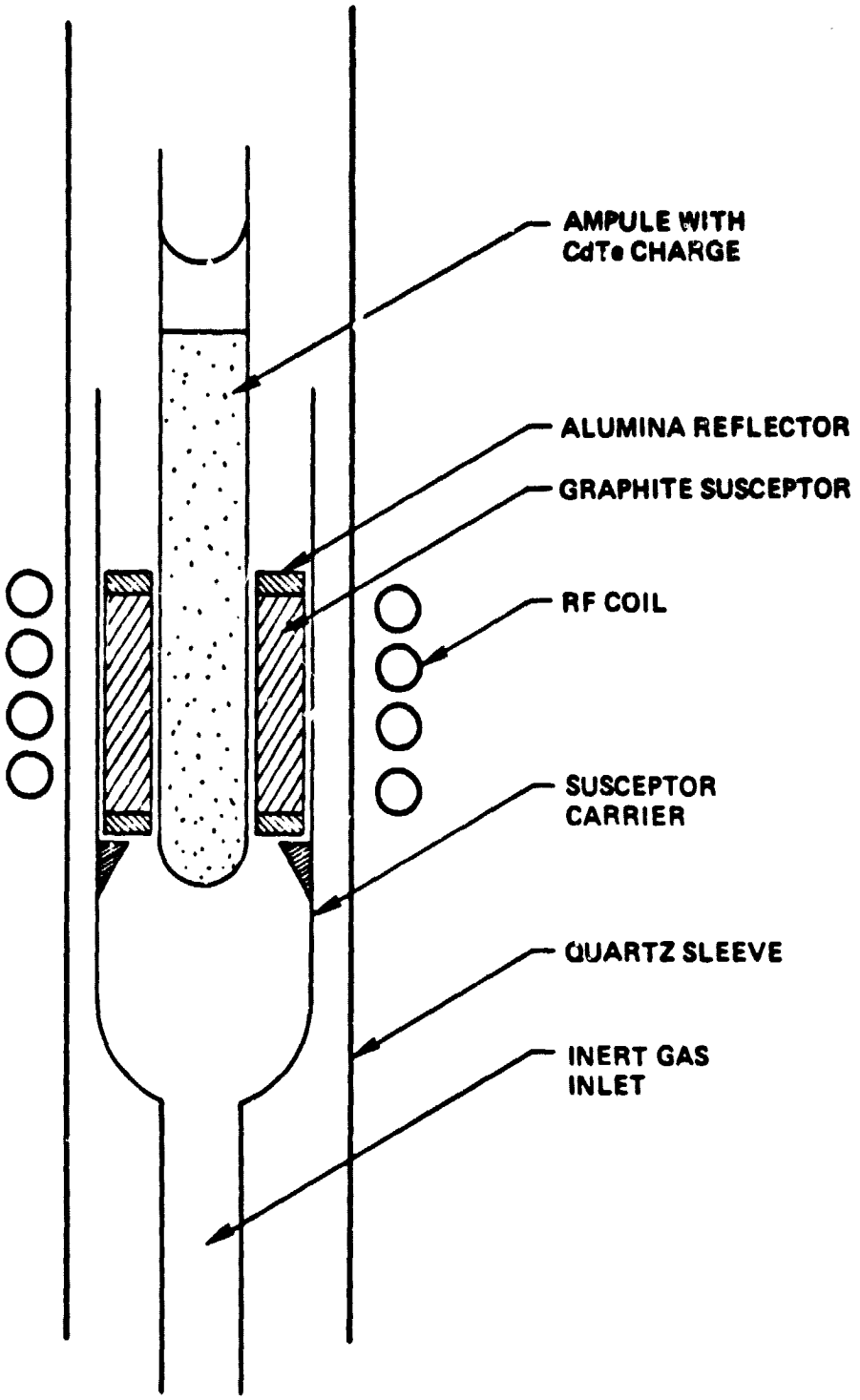

Fig. 20 Traveling zone - graphite susceptor approach.

graphite (quartz sleeves and a flow of nitrogen gas) while adequate to prevent the rapid disintegration of the graphite susceptor, allowed a slow degradation to occur causing temperature variations due to changes in coupling efficiency. Also temperature inomogeneities arose due to preferential attach of the graphite. Second, direct observation of the molten zone was not possible, making it difficult to determine the true temperature of the hot CdTe zone. Using excess power could ensure a liquid zone, but increase the possibility of ampoule rupture due to the rapidly rising cadmium vapor pressure. Results using the above susceptor arrangement were poor. Typically, complete melt through of a 15 mm diameter CdTe rod was not achieved since temperatures could be inferred only from the outer susceptor surface. Also, there was evidence that the molten zone was not uniform - one side of the zone being higher than the other. This was due to either susceptor degradation or a nonuniformity in the nitrogen gas flow around the susceptor causing local cooling and thus temperature inhomogeneities.

In view of these difficulties with the indirect heating method alternative approaches to melting and maintaining a liquid CdTe zone were initiated. Direct coupling between the RF and CdTe should be possible provided the CdTe can be made liquid or at least hot enough to become sufficiently conductive to allow coupling. To preheat the CdTe, the following arrangement was used. Again a conductive susceptor made, however, out of Inconel (a high nickel content alloy), was used to preheat and liquify part of the CdTe charge. Since Inconel has relatively high oxidation resistance at high temperatures, the usage of enclosures and inert ambient required with a

graphite susceptor became unnecessary, simplifying the experimental setup. The melting point of Inconel is 1400°C, sufficiently high to melt CdTe which melts at 1090°C.

Initial attempts consisted of preheating approximately 1 in. of the CdTe charge with the Inconel susceptor, quickly removing the susceptor, and allowing direct coupling between the RF and hot CdTe to occur. Successful coupling occurred only in those cases where the CdTe was already liquid, no coupling occurred to hot solid CdTe. These experiments were made difficult by the "one shot" nature of the experiments. If direct coupling did not occur to the molten CdTe when the suceptor was removed, the ampoule would crack upon the solidification of the CdTe, necessitating the preparation of a fresh ampoule. Coating the ampoule with pyrolytic graphite via pyrolysis of methane reduced the breakage of the ampoule, but did not entirely eliminate it.

The CdTe charge was prepared as follows: a 15 mm × 18 mm quartz ampoule was cleaned and coated with a thin layer of pyrolytic graphite obtained by the pyrolysis of methane at high temperatures. This film was thin enough to allow visual observation of the liquid yet preventing "wetting" of the quartz by the molten CdTe and eliminated the cracking of the ampoule upon solidification of the CdTe. The ampoule was then filled with crushed CdTe material taken from a Bridgman grown boule. To compact the charge, the ampoule was then placed inside a 6 in. long Inconel sleeve and the entire ampoule brought above the melting point of CdTe via RF heating of the Inconel sleeve. Subsequent to this step, the long Inconel sleeve was replaced by a 1 in. high sleeve and a four-loop 1.2 in. diameter RF coil at the bottom end

of the ampoule. Approximately, one inch of charge was preheated and liquified by the Inconel sleeve, which was then removed. Fig. 21a shows the liquid zone about one minute after removal of the Inconel sleeve and after direct coupling between the RF power and molten CdTe had occurred. The zone immediately doubled in size, going from one to two inches in length. Very strong and turbulent convection currents were observed. Figures 21b and 21c are photos of the molten zone taken through the lens system of an IRCOM IR pyrometer with a Polaroid Land camera. Although the convection currents are not distinct because of insufficient film speed the photos show some of the temperature variations due to convection currents. Measuring the temperature variations with an uncalibrated IRCOM pyrometer indicated a range from 1140°C to 1190°C - a fifty degree spread. Also, zone length stability was poor, apparently due to the destabilizing nature of the coupling. If the molten zone increases, coupling efficiency improves leading to an even longer zone. However, with a decreasing zone, coupling efficiency decreases causing rapid collapse of the zone. Indeed, if the temperatures as measured with the IRCOM pyrometer could be trusted, the entire experiment had to be run with a molten zone considerably higher in temperature than necessary (1140-1190°C) to melt CdTe (1090°C). Attempts to operate with smaller power inputs to achieve a smaller zone and lower temperatures failed due to a slow decrease in coupling efficiency and subsequent freezing of the zone. Continuing the experiment with a large two inch zone, it also became apparent that the zone was not symmetric with respect to the RF coil. Figure 21d shows the experiment three hours after initiation and 3/4 of an inch of travel - the liquid zone extends

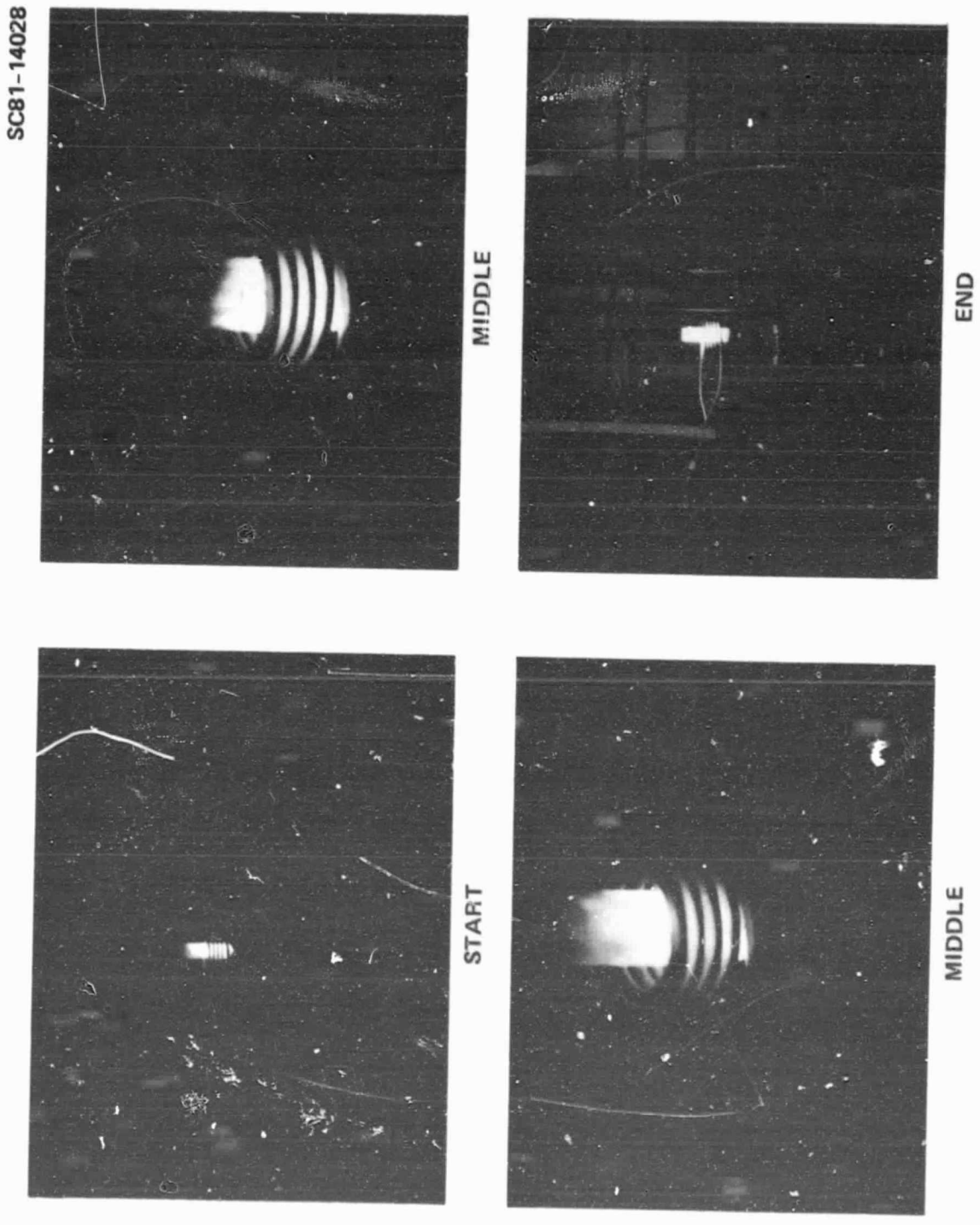

Fig. 21 Molten zone - direct RF coupling.

1 in. above the RF coil, but only about 1/4 of an inch below the coil. No satisfactory explanation could be found for this behavior, however, thermal convection was felt to be the main cause of the zone asymmetry.

Having successfully established a liquid zone via direct coupling the main effort was then directed at reducing the zone length and increasing zone stability. To study the effect of a number of turns in the RF coil on the zone length an attempt was made to establish a liquid CdTe zone using one turn RF coil. This attempt was not successful - susceptor temperature sufficiently high to allow direct coupling to the CdTe could not be achieved because of insufficient power. Use of a two turn RF coil of the same diameter, 1 inch, allowed the Inconel susceptor to become hot enough to allow direct coupling to occur. Upon removal of the susceptor, i.e., direct coupling mode, the liquid zone increased approximately 2 inch in length. The power level was decreased until the zone length reached approximately 1 inch At that point the linear motion of the ampoule through the RF coil was started at a rate of 0.5 in./hr. After fifty minutes, approximately one half inch of travel, CdTe solidification at the ampoule tip was observed and concurrently liquid zone length decreased. With continued travel and solidification of CdTe zone length continued to decrease until after 1 in. of travel the zone froze despite a continuous increase of input power. There are two possible reasons for this behavior. First, the heat sinking effect of the solidifying CdTe; heat being removed from both ends of the liquid zone by the solid, may be sufficient to cause slow decoupling with the limited flux of a two turn coil at the power levels possible with the current RF generator (10 kW). This

behavior was not observed with the higher flux density of the four loop coil used in previous attempts. A second reason may have possibly been a inhomogeneous CdTe charge caused by Cd loss during the initial melt down and compacting of the crushed CdTe charge. This would have lead to compositional gradients and thus varying melting temperatures along the charge thus possibly explaining the observed zone behavior.

While the use of a two loop RF coil reduced the zone length to approximately one inch, this was considerably more then could be expected to be self supporting via surface tension in a free standing zone; thus an effort was undertaken to explore the use of the "split" susceptor technique as an alternative heating method to establish a uniform and stable liquid CdTe zone. In addition, further motivation for exploring an alternative heating method was that zone stability in the direct coupling mode was poor; rapid zone length changes and turbulent fluid flow being the main destabilizing agents.

With the "split" susceptor technique partial coupling occurs to both the susceptor and the CdTe liquid. The susceptor itself is similar to the design used in the direct coupling mode except that a one mm gap is cut into the perimeter along its length. Also the length was reduced to 1/2 of an inch for the initial attempts to ensure high enough temperatures could be reached with the available power and limited flux of a two loop RF coil.

Initial attempts using this susceptor design resulted in failure mainly due to deformation of the susceptor at high temperatures and errosion

caused by sparking across the gap. Increasing the gap and improving the mechanical support of the susceptor with a redesigned quartz sleeve led to the successful melting of a fifteen mm CdTe rod. The experimental procedure consists of locally preheating the CdTe rod with the RF heated susceptor until direct coupling occurred. At this point, however, the susceptor is not removed as in the direct coupling mode. Upon direct coupling with the split susceptor/coil arrangement the CdTe liquid zone rapidly increases until the zone was approximately twice as long as the susceptor. Such a zone is shown in Fig. 22. Note that the susceptor is considerably colder than the liquid CdTe as can be inferred from the color difference indicating that coupling efficiency is considerably higher to the liquid CdTe than to the Inconel susceptor. Zone characteristics in this mode are similar to those observed with the direct coupling technique - strong, turbulent convection and asymmetry of the zone with respect to the coil/susceptor as can be seen in Fig. 22 where the zone extends considerably above but not below the susceptor. Reducing power levels to reduce the zone length lead to a slow collapse of the zone similar to that observed in the direct coupling mode since the susceptor is not hot enough, due to less efficient coupling than to liquid, to keep the CdTe conductive.

Plans for a more detailed investigation of this technique were not carried out due to the ending of this contract. Of the heating techniques considered and tested the split susceptor geometry appears the most promising, however, primary importance will need to be the equalization of the temperature of the susceptor and that of the liquid zone. With such an

SC81-14036

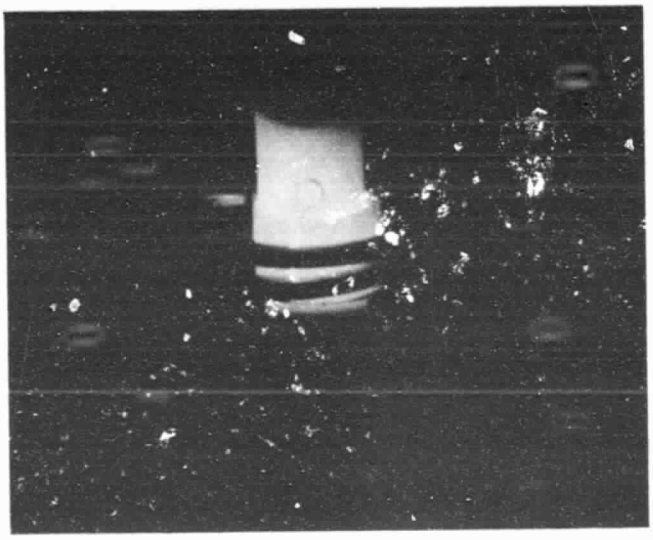

Fig. 22 Liquid zone established via partial RF coupling.

arrangement a uniform, stable and small (5 mm) CdTe liquid should be obtainable.

5.3 Material Analysis

A total of seven growth runs were attempted on this program. Detailed analysis of the material grown was not carried out since the main effort lay in the CdTe charge preparation and finding a heating technique that would result in a stable liquid zone.

Following is a description of the analysis of growth attempt number seven grown by the "split" ring susceptor arrangement. Results obtained for this ingot were shared in general by all the other material grown in this program under various charge preparations and zone melting methods.

The ampoule containing the grown material is shown in Fig. 23. Liquid-solid separation occurred after approximately 5 cm of growth due to loss of Cd and CdTe from the liquid zone. After removing the grown material from the ampoule it was sandblasted to reveal grain structure. Visual observation of the grain structure on the surface of the ingot indicated high polycrystallinity. This was confirmed by cross-sectioning the grown ingot parallel to the growth axis as shown in Fig. 24, where the grain structure can be seen to exist throughout the whole volume of the ingot. The quenched liquid-solid interface is indicated by an arrow in Fig. 24. The high polycrystallinity is probably caused by the high thermal gradients of the

SC81-14033

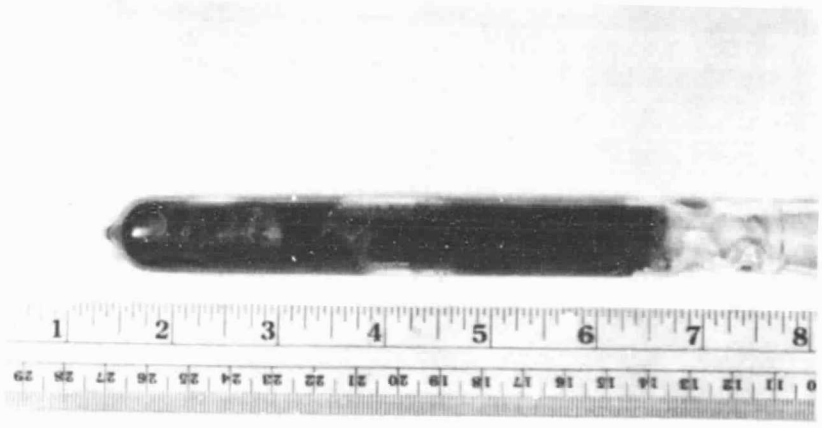

Fig. 23 CdTe growth attempt No. 7.

SC81-14034

Fig. 24 Cross-section CdTe growth attempt No. 7.

travelling zone growth method, which lead to turbulent convection currents and, consequently, spurious nucleation and sub-grain formation.

Indeed all of the material grown in this program were highly polycrystalline. Figure 25 is a cross-section of growth attempt No. 4 grown in the direct coupling mode which also shows the same general structure as growth No. 7.

X-ray analysis was not carried out since visual observation indicated a large randomness in growth orientation. Part of the material was polished chemomechanically to allow the infrared transmissivity to be taken. This is shown in Fig. 26, where the IR transmissivity versus wavelength for CdTe No. 7 material is shown. The 100% reference signal is at the top of the chart. The maximum transmission for CdTe without antireflection coting (conditions under which this data was taken), is approximately 64%. The roll-off at 11 μm is due to instrumental problems as can be seen in the drop of the reference signal. An approximate 5% drop in signal level (reference signal rises 5% between 2.5 μm and 10 μm) would indicate free carrier absorption due either to an impurity background or a stoichiometric defect. The reason for the dip in the signal level at 7.8 μm is unknown at this time.

Another technique that was used to characterize the material was IR microscopy. Here the bulk of the sample can be examined. This technique reveals bulk macrodefects such as inclusions and impurity decorated low and major grain goundaries. Figure 27 shows IR microscopy results for growth No. 7.

SC81-14031

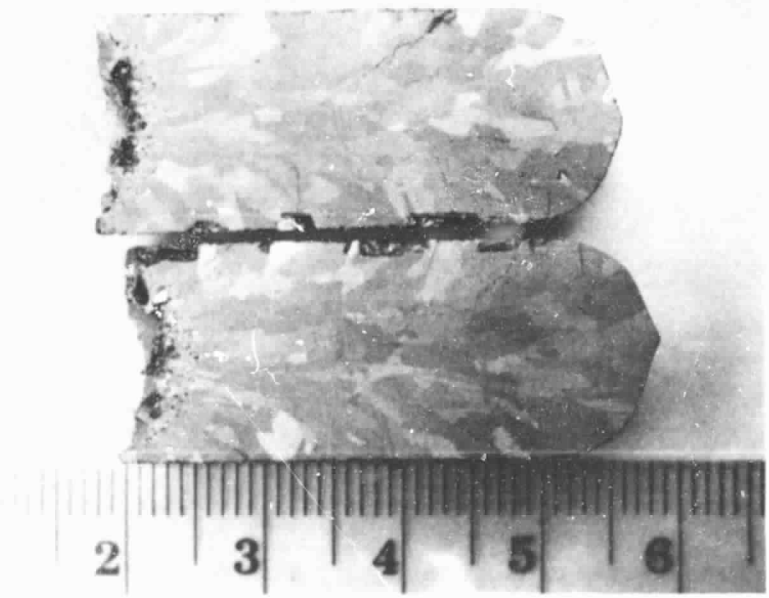

Fig. 25 Cross-section growth attempt No. 4 direct coupling mode.

SC81-14029

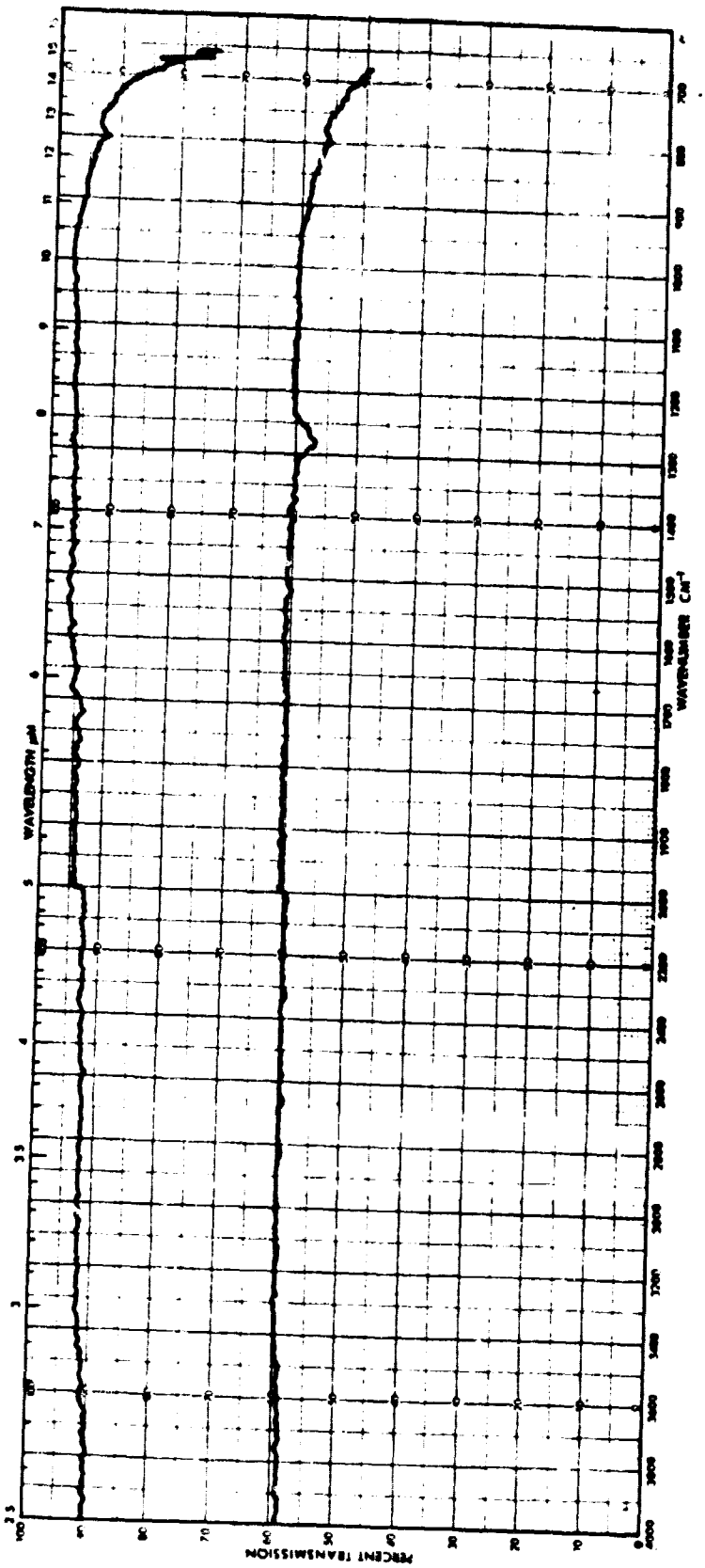

Fig. 26 300K IR transmissivity of zone grown CdTe No. 7.

SC81-15521

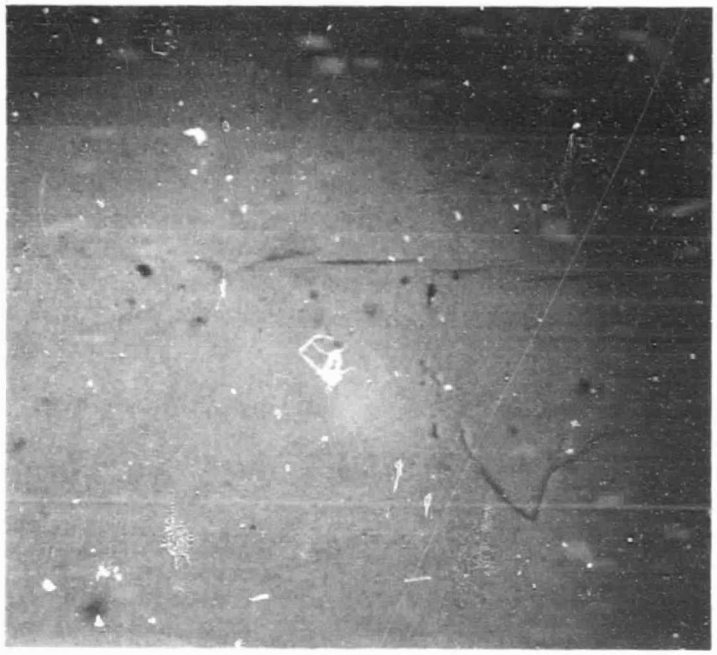

Fig. 27 IR microscopy of CdTe No. 7.

Etch pit studies to establish dislocation density concentrations were not carried out since well-oriented material is necessary for the known dislocation etches to be effective.

5.4 Conclusions and Recommendations

During the course of this program it has become apparent that the successful zone melting of CdTe will necessitate the use of a scaling cap to prevent loss of Cd and CdTe from the molten zone. Using boric oxide or other fluxes to prevent vapor losses considerably complicates the experimental setup since the oxide must be kept above its liquidus point in order to prevent it from cracking the quartz ampoule upon solidification.

Also, effect of the cap on interface shape, and compositional uniformity (potential solubility of Cd and/or Te in the cap) will need to be established.

The RF heating techniques used in this program resulted in large, nonuniform and unstable liquid zone. However, the most promising technique, the split ring susceptor arrangement, was not fully investigated in this program and needs further investigation.

All the CdTe material grown in this program was highly polycrystalline which was not surprising considering the unstable nature of the RF heated liquid zone. The synthesis of single crystal CdTe by a zone melting technique will depend critically on the development of a heating method that will yield a stable uniform liquid zone.

6.0 REFERENCES

1. W. G. Pfann, Trans. AIME 194, 747 (1952).

2. W. Heywang, Z. Naturforsch. 11A, 238 (1956).

3. A.F. Witt and H.C. Gatos, J. Electrochem. Soc. 113, 808 (1966).

4. A.F. Witt, H.C. Gatos, M. Lichtensteiger, M.C. Lavine and C.J. Herman, Proc. of the 3rd Space Symp. of Skylab, NASA TMX-70252 (1974).

5. A.M. Andrews, D.T. Cheung, E.R. Gertner, and J.T. Longo, J. Vac. Sci. Technol. 13, 961 (1976).

6. R. Triboulet, Y. Marfaing, A. Cornet and P. Siffert, J. Apply Phy., 45, 2759, (1974).

7. R.O. Bell, N. Hemmat, and F. Wald, Phys. Stat. Sol. (a) 1, 375 (1970).

8. J.B. Mullin and B.W. Straughan Rev. Phys. Appliquee, 12, 105 (1977).

9. K. Zanio, J. Elect. Mat. 3, 327 (1974).

10. B. Lunn and J. Bettridge, Rev. Phys. Appliquee, 12, 151 (1977).

11. K. Zanio, Semiconductors and Semimetals, Vol. 13, Academic Press, 1978, (eds., R.K. Willardson and A.C. Beer).

12. ibid, p. 6.

13. A.J. Strauss, Proc. of Int. Sym. on Cadmium Telluride, Strasbourg, 1971, Eds., P. Siffert and A. Cornet, Centre de Recherches Nucleaires (publishers).

14. J. Drowart and P.J. Goldfinger, J. Chem. Phys. 55, 721 (1958).

15. P.J. Goldfinger and M. Jeunehomme Trans. Faraday Soc. 59, 2851 (1963).